

Reply to reviewer comments

Dear Editor,

Please find below our point by point response to the comments of the reviewers (*reviewer, response*). We thank both anonymous referees for the time and effort in reviewing our manuscript (cp-2020-39). The comments, suggestions and feedback raised in the review are highly appreciated as they help us to clarify our statements and to improve the quality of our manuscript. In our response, we have highlighted the relevant changes made in the manuscript with **line numbers**. Furthermore, we have attached a marked-up manuscript version.

On behalf of all co-authors, I would like to thank the Editor.

Best regards,

Daniel Balting

Anonymous referee #1

By analysing a European network of 26 tree-ring sites with $\delta^{18}O$ measurements, the authors aim at extracting regional climate signal imprinted in the records to investigate the dominant modes of variability of the European climate and their relationships with the large-scale atmospheric circulation, in particular ENSO. Their findings suggest that climate variability in Europe is strongly modulated by ENSO teleconnections at least over the past 130 years, but that some differences arises between the northern and southern regions.

Although the results are promising, I do not think the manuscript is ready for publication yet. A restructuration and reorganisation of the paper is strongly needed. While the introduction is relatively well written and easy to follow, many confusions arise from the Material and Methods section and some clarifications are required to allow the readers to easily understand why and how the proposed analyses were made. The division of the 'Results and Discussion' section into two separate sections should improve the readability of the manuscript. It seems that the authors have not carefully re-read their manuscript to check for typos and ensure that the text is fully understandable before submitting it. The authors also should make an effort to properly, clearly and thoroughly discuss their results and their implications for the understanding of the atmospheric teleconnections. So far only in the Summary and Conclusion section are the results clearly highlighted and interpreted.

R: We are glad that the results are promising, and we agree with the reviewer that structural changes are necessary. Therefore, the "Material and Methods" section have been sustainably revised by a more detailed description of the isotope measurements and of the used climate data including the used ENSO indices and the SST dataset as well as an extended explanation of the used methods [section 2].

Furthermore, we have separated our discussion from the results section. The comparison to other studies and the implications of our results have been worked out more in detail [section 3 & 4].

Some additional comments and suggestions:

L20: 'may not be stable. . .'

R: We have added the missing word [L20].

L42-43: *Actually, it is the other way around: $\delta^{18}\text{O}_{\text{Ocel}}$ depends on $\delta^{18}\text{O}_{\text{OSW}}$ but $\delta^{18}\text{O}_{\text{OSW}}$ itself does not depend on $\delta^{18}\text{O}_{\text{Ocel}}$. Please rewrite.*

R: Thank you for the comment! We have fixed it in the revised version of the manuscript [L40-41].

L55-56: *You could also cite more papers showing the potential of $\delta^{18}\text{O}_{\text{Ocel}}$ for reconstructing large-scale patterns of climate variability (since it is one aim of your study), e.g.: Brienen, R. J. W., Helle, G., Pons, T. L., Guyot, J.-L., Gloor, M., Oxygen isotopes in tree rings are a good proxy for Amazon precipitation and El Niño-Southern Oscillation variability, *PNAS*, (42) 16957-16962; DOI: 10.1073/pnas.1205977109, 2012 Lavergne, A., Daux, V., Villalba, R., Pierre, M., Stievenard, M., Srur, A. M., Vimeux, F., Are the $\delta^{18}\text{O}$ of *F. cupressoides* and *N. pumilio* promising proxies for climate reconstructions in northern Patagonia?, *J. Geophys. Res.-Biogeo.*, 121, 767-776, <https://doi.org/10.1002/2015JG003260>, 2016.*

R: The suggested references have been implemented into the revised manuscript [L53-54].

L76-77: *I am not sure what is the meaning of this sentence. Please rewrite. L75-80: I would suggest clearly rewriting this part as it is difficult to read. You should get right to the point: how are you going to achieve your goals? What are the main analyses you are going to perform to reach those goals?*

R: We agree with the reviewer that the last paragraph of the introduction was difficult to read. According to the comment of the reviewer, we have rewritten the entire paragraph and have highlighted the goals and methods to reach our goals [L71-77].

L94-96: *Please comment on the implication of only using latewood for oak but both early- and late- woods for the coniferous species. Are you suggesting that earlywood in the coniferous species is only derived from carbohydrates formed during the current year? Please rewrite the sentence accordingly.*

R: Basically, trees form their annual ring from current assimilates and reserves (starch and fats). The used carbohydrates come from a pool which, depending on the season and the rate of assimilation during the vegetation period, is in part clearly dominated by reserves from the previous year(s). Since the conifers of the isotope network are evergreen, the proportion of the reserves used for wood accumulation decreases rapidly at the beginning of the earlywood formation and is usually not as high at the beginning as in the case of the deciduous oak trees utilized here. Therefore, we don't suggest that earlywood is only derived from carbohydrates formed during the current year for coniferous. However, oak is a ring-porous tree species

known for having its earlywood growth almost completing before the leaves are fully green and net photosynthesis is positive. Hence, for this species it makes sense to skip earlywood as it is rather easy to distinguish from latewood. On the other hand, it is difficult to identify a clear boundary between the early- and latewood of conifers without technical means of quantitative wood anatomy. We have implemented our comment in a short version in the revised version of the manuscript [L95-97].

L100-101: "Here" is repeated twice in the sentence. Furthermore, the sentence is not grammatically correct. Please be more careful!

Erroneous repeating of the word "here" has been fixed as well as the sentence has been grammatically corrected [L101-102].

L108-109: what is the COBE-SST₂ dataset? Please describe it here. Also, which index of ENSO are you using to define El Niño/La Niña years?

R: We agree with the reviewer that the used SST dataset should be explained more in detail [L114-119].and also the ENSO index is now presented in this subsection [L122-129]. In the revised version of manuscript, we have revised the entire section and have added arguments why we used the climate data [subsection 2.2].

L114-116: What is a 'nudge model scenarios/simulation'? It is not clear why you choose this title for the section. I would recommend combining sections 2.2 and 2.3 instead. How using both $\delta^{18}O_P$ and $\delta^{18}O_{SW}$ will inform you about 'fractionation/ photosynthesis processes'? You will never get insights into the fractionation processes occurring during photosynthesis using only those two timeseries! Please clarify.

R: We thank the reviewer for pointing out that the subsection a 'nudged model scenarios/simulation' was not well explained and also confusing. In general, the name of the chapter is given based on the method which produces $\delta^{18}O_P$ and $\delta^{18}O_{SW}$ (in our case the nudged model simulations from Butzin et al. (2014)). Our goal with the model output is to test the correlation between $\delta^{18}O_{cel}$ and modelled $\delta^{18}O_P/\delta^{18}O_{SW}$ to identify if the water, which is used within the photosynthesis processes, has a multi-seasonal isotopic signature. If yes (as shown in our plots), it is an explanation how $\delta^{18}O_{cel}$ is able to capture the ENSO signal. Based on the questions and suggestions of the reviewer, the subsection has been renamed and sustainably changed with a better explanation of the technique behind and an argumentation why we used the model output [subsection 2.3].

L123-131: What is the difference between EOF and PCA? From my understanding of those analyses, EOF and PCA are really similar. Are you suggesting that EOF provides information about spatial patterns, while PCA gives information about temporal patterns? The whole paragraph is confusing (especially the filtering actually done to fulfil the North et al. (1982) rule), please rewrite.

R: Overall the PCA and EOF technique are related, but differences exist and both abbreviations are often mixed up. Based on the comments of both reviewers, we have rewritten our explanation of the PCA and EOF technique. Furthermore, we have added a more detailed explanation of the North et al. (1982) rule [L153-170]. After this paragraph we will add a simple explanation about PCA and EOF analysis.

The concept of the Principal Component Analysis (PCA) was firstly described by Pearson (1902) and Hotteling (1935) and used for the first time by Lorenz (1959) for climatological research (Storch & Zwiers, 1999). The general aim of the PCA is to find a new set of axes which explains the most of the variability within the dataset. This is done by rotating the initial data onto axes which are orthogonal to each other (Schönwiese, 2013). For this purpose, a vector is necessary which indicates the direction of the new coordinate axis which is called eigenvector. This type of vector doesn't change its direction by a rotation. Therefore, the eigenvectors are used as a transformation matrix for the input high dimensional datasets onto the new axis. To indicate if a rotation maximizes the explained variance, every eigenvector has a corresponding eigenvalue. The corresponding eigenvalue is a kind of stretch factor for the eigenvectors. A huge eigenvalue indicates that the eigenvector has to be strongly stretched to map high variabilities within the dataset which can be explained with the new set of axes. Therefore, the eigenvalue (λ) is equal to the variance of the time series (\vec{X}) from matrix M which got rotated by the corresponding eigenvector (\vec{e}) (Equation 1).

$$Var(\langle \vec{X}, \vec{e} \rangle) = \lambda \quad (1)$$

To find a first set of eigenvalues and eigenvectors, the data is rotated until an axis can be defined which explains the highest variance. Storch & Zwiers (1999) described this with the effort of minimizing ϵ_1 respectively to maximize $Var(\langle \vec{X}, \vec{e}^1 \rangle)$ (Equation 2).

$$\epsilon_1 = Var(\vec{X}) - Var(\langle \vec{X}, \vec{e}^1 \rangle) \quad (2)$$

Finally, the rotated data forms the first component. Like in a traditional coordinate system, it is possible to calculate a new axis which is orthogonal to the first one. Therefore, the second component is formed by an orthogonal rotation around the axis of the first component. The total number of components is given by the absolute number of time series. To compute the time series for the first component, the e.g., first value of all input time series is multiplied

with the individual eigenvector and afterwards, summed up over all time series for each year. This process forms the time series of a principal component which has the same temporal coverage as the input time series.

Especially a separate analysis of the eigenvectors of \vec{X} is commonly used. This analysis is known as Empirical Orthogonal Functions (EOF) and the goal of it is to identify spatially coherent climate patterns which explain a significant part of the variance for a specific region (this is shown and used for example in Ionita et al. (2008)). Therefore, the largest part of the variance can be explained by the pattern of the leading EOF.

L132-133: Why are you mentioning this here? It should be already stated in Section 2.1.

R: It is mentioned here again to explain why we used the filling algorithm of Josse and Husson (2016).

L133-140: How can you be sure that by using the gap fill method, you will not influence your results? Also, why would you need to fill in the gaps for 400 years knowing that your climate data only goes up to 1851?

R: Since the used climate data is only available from 1851, the advantage of using the presented tree ring network is to go beyond this time scale and to introduce a new perspective on the observed relationship between $\delta^{18}\text{O}_{\text{cel}}$ and ENSO activity back in the past. If we want to go back in the past the filling algorithm is necessary because the temporal coverage of the $\delta^{18}\text{O}_{\text{cel}}$ records is different as described in the "Material and Method" section.

We agree with reviewer that the gap filling method needs to be better evaluated. In the revised version, we have added a new section in the methods [179-183] and in the results [L244-L254] which contextualizes the uncertainties of the used gap filling method.

L141-146: What do you mean? The whole paragraph is pretty confusing and after reading it several times, I still do not get what you are really doing here.

R: Thanks to reviewer for highlighting this point. We agree that our explanation of the composite maps has potential for improvements. In the revised version of the manuscript, we have rewritten and supplement our explanation of the composite maps [L184-190]. Furthermore, we have changed the corresponding figures to show the difference for high and low values of PC1 for SST and Z500 [Fig. 4 & 5].

What kind of information is providing the geopotential height 500mb (Z500) for the analysis?

R: The geopotential height is a standard variable in atmospheric sciences which is often represented in contour maps with isohyets. They connect places at the same altitude at which a certain air pressure (here 500 hPa which is on average 5500 meters high) prevails. This height is called geopotential in meteorology. With the differences in the geopotential height maps, it is possible to identify low- and high-pressure systems based on the different pressure patterns as for example shown in Figure 4. From the Z500 maps, the wind direction can be determined which is helpful for the understanding and the investigation of large-scale flows in the atmosphere. A big advantage of this variable is that the influence of friction at the surface and the influence of dynamic disruptive factors of the upper layers of the atmosphere, e.g. the Jetstream, are relatively minor.

L151: 'Nino 3.4 index' this should come earlier in section 2.2 when you are presenting the environmental data used in the analyses.

R: We agree with the reviewer and we have shifted the explanation of Nino 3.4 index to the explanation of the used climate data [L122-124].

L158-160: The first sentence does not provide any clear information. Please remove.

R: The highlighted sentence has been removed in the revised version of the manuscript.

Figure 1: Could you add more information in the figure A related to the latitude of each site? The names and characteristics of the sites are not presented anywhere in the manuscript. Even though the data have already been published, a Table with sites information should be included. In figures B and C, how is it possible that R2 and p-value are exactly the same for the relationships between $\delta^{18}O_{cel}$ and altitude and between $\delta^{18}O_{cel}$ and latitude? I suspect that there is a mistake here.

R: We agree with the reviewer that more information about the sample sites would be helpful. Therefore, we have added a table with the coordinates, tree type and altitude for each site in the revised version of the manuscript [Supp. 1]. Furthermore, the reviewer is right that there is a mistake within the textbox of Figure 2B (should be $R^2=0.417$ and $p\text{-value}=2.17e^{-04}$) of submitted manuscript. That has been fixed in the revised version of the manuscript [Fig. 2].

L160-161 and L172-173: Since no information about the exact location of the site presented in Figure 1A is provided, it is difficult to follow this statement.

R: We agree with it. It will be easier to understand in the revised version of the manuscript, because of the added table which contains the characteristics of each sample site [Supp. 1].

L162: I would remove 'This might be determined genetically,' from the sentence as it is not completely accurate (different species of *Quercus* also have different genetic information).

R: We thank the reviewer for that suggestion, and we have removed that part.

L165: You could also cite more updated papers describing differences between angiosperms and gymnosperms, e.g.: Carnicer J., Barbeta A., Sperlich D., Coll M., Penuelas J., Contrasting trait syndromes in angiosperms and conifers are associated with different responses of tree growth to temperature on a large scale, *Front. Plant Sci.*, 4, 409, <https://doi.org/10.3389/fpls.2013.00409>, 2013

R: The mentioned reference has been integrated in the revised version of manuscript [L. 209-210].

L177: 'which could influence the relation by a latitudinal effect.' please rewrite as 'thus the latitudinal and altitudinal gradients may have confounding effects on $\delta^{18}\text{O}_{\text{cel}}$ ' or something similar

R: Thanks to reviewer for that comment. We have rewritten this sentence according to the suggestion of the reviewer [L220-221].

L177-179: I would rewrite this sentence as the effects of the two gradients on $\delta^{18}\text{O}_{\text{cel}}$ have already been observed and documented in many other studies, for instance: Szejner, P., W. E. Wright, F. Babst, S. Belmecheri, V. Trouet, S. W. Leavitt, J. R. Ehleringer, R. K. Monson, Latitudinal gradients in tree ring stable carbon and oxygen isotopes reveal differential climate influences of the North American Monsoon System, *J. Geo-phys. Res. Biogeosci.*, 121, 1978–1991, doi:10.1002/2016JG003460. 2016

R: We have rewritten the sentence [L221-222] and have added a new subsection to discuss the effects of latitude and altitude $\delta^{18}\text{O}_{\text{cel}}$ [subsection 4.1].

L181-186: Here again comes the confusion between EOF and PCA. You should clarify from the beginning (see previous comment) what is the difference between the two especially given that EOF1 and PC1 both seem to explain 16.2% of the variance in the records.

R: We see the point that the differences between EOF and PCA is not well explained and can be confusing in the submitted manuscript. With the new explanation [L153-170], it will be easier to understand the differences.

Figure 4: In the legend, you are describing the columns not the rows.

R: Thank you for the comment. Since we have added new figures, the figure captions have been updated [Fig. 4].

L216 Is the distribution of PC₁ for El Niño (or La Niña) years significantly different from that during normal years (i.e. when excluding El Niño/La Niña years)?

R: Yes. This is shown in Supp.3. To make it easier to understand, we have rewritten this part in the revised version of the manuscript [L286-290].

L222-224: Please rewrite the sentence. As it reads now, it looks like you are saying that Europe is characterized by higher precipitation and lower air surface temperatures in summer! And it is not clear what the parentheses apply for.

R: We agree with the reviewer that the explanation of the composite maps can be confusing. The updated explanation of the composite maps [L184-190] and the new figures [Fig. 4,5,6,8,9] in the revised version of the manuscript will make it easier to follow and to understand our argumentation.

L230-231: 'because we to take into account. . .' Why would SPEI₃ index accounting for the climate conditions prevailing over the previous season? So far, nothing has been said about this dataset.

L227-233: this part mostly belongs to the Material and Methods section and could be improved for readability.

R: We have added more details about the SPEI₃ dataset within the Section 2.2 [L110-113] and have removed the explanation from the results subsection.

L235: 'the used reconstruction': which one?

R: Thanks to the reviewer for highlighting the point that it is not clear which reconstruction was used. We have rewritten the sentence and have added the reference of the used reconstructions [L294-297].

L240: 'to capture a multi-seasonal signal' what do you mean?

R: We agree with the reviewer that this part is not easy to understand. We have revised that part [L299-300] and have added further information about the goal and method of nudged model simulations [subsection 2.3].

L243-244: where is it shown?

R: This is shown in [Figure 7](#) of the revised manuscript.

L244-245: so why then $\delta^{18}\text{O}_{\text{cel}}$ is not more strongly related to $\delta^{18}\text{O}_{\text{sw}}$? Your argument is contradictory with what is actually described.

R: We thank the reviewer for the helpful comment! The referred sentence is difficult to understand and we have rewritten it [[L304-305](#)].

L239-248: And so what? What are you really trying to say here? Also, I do not think the results are properly discussed and compared to the literature.

R: We agree with the reviewer that the results should be compared to literature and discussed more thoroughly. In the revised version of the manuscript, we have added a subsection to discuss the winter climate signal in $\delta^{18}\text{O}_{\text{cel}}$. Furthermore, we have highlighted our implications of our results [[subsection 4.4](#)].

Figure 6: You mean the upper row Why description of Figure 6 comes before Figure 5?

R: Thank you for the suggestion. Yes, we do mean the upper row; we have changed the figure caption accordingly [[caption of Fig. 7](#)]. Furthermore, we have changed the order of the figures.

L168-169 and L276: Please rewrite sentences

R: We have rewritten the mentioned sentences [[L210-212](#), [L444-445](#)].

*L236-237: The instability of the relationship between climate variables and ENSO has also been documented by other tree-ring studies in southern South America, e.g: Álvarez, C., Veblen, T.T., Christie, D.A., González-Reyes, Á., Relationships between climate variability and radial growth of *Nothofagus pumilio* near altitudinal treeline in the Andes of northern Patagonia, Chile. For. Ecol. Manage. 342, 112–121, 2015*

R: The suggested reference has been implemented in the revised version of the manuscript [[L371](#)]. Furthermore, we have added a subsection to discuss the stability of the ENSO signal [[subsection 4.3](#)].

Anonymous referee #2

Summary

The authors investigate $\delta^{18}O$ tree ring records of 26 sites distributed over Europe for the last 400 years. They claim that they were able to identify a connection of the leading mode of variability of this data to El Niño Southern Oscillation. They speculate that this connection is only found in the last 130 years and thus the connection is not stable in time. The second mode of the data is suggested to reconstruct regional summer atmospheric circulation. Finally, the author team claim that $\delta^{18}O$ tree ring records can be used to reconstruct atmospheric circulation.

General comments

The topic would certainly be of high interests. However, the authors fail to convincingly show evidence for their main claims listed in the summary. Therefore, I recommend to reject the manuscript.

Major comments

1. At several places in the manuscript the authors claim that their analysis suggests "the relationship between ENSO and the European climate may not stable over time". The connection is only found for the instrumental period after 1850 CE. I think the first order interpretation is that the reconstruction of ENSO might be not perfect, as normally the reconstruction methods are trained in the last 100 to 150 years. So differences between the training periods and the period before are a hint that the reconstruction might be not successful. So, from your analysis you cannot conclude that you have identified non stationarity of teleconnections.

R: We thank the reviewer for this comment. It stresses that we have to put further work into the manuscript clarifying our results and interpretations as we are not intending to say that we have identified a non-stationarity teleconnection. We only say that the correlations and coincidence rates are weakening, which indicates that the relationship between PC₁ of the $\delta^{18}O_{\text{cel}}$ network and ENSO might not be stable over time. Therefore, we can only suggest that the relationship between ENSO and the European climate may be not stable over time which is supported also by other studies based on proxy data (e.g., Rimbu et al., 2003). The idea of a unstable relationship is also supported by the results from studies based on instrumental data (e.g. Fraedrich, 1994; Fraedrich and Müller, 1992; Pozo-Vázquez et al., 2005) or studies based on ocean-atmosphere coupled models (e.g. Raible et al., 2004; Deser et al., 2006; Brönnimann et al., 2007) The fact that the relationship between climate variables

and ENSO is not stable over time has been also recognized in tree-ring studies in other regions, e.g. South America (Álvarez et al., 2015). Nevertheless, we are aware of the fact that further research is necessary to make a confident statement.

It is true that reconstructed ENSO indices before instrumental period are not perfect which could be the cause of decrease in the correlations between our PC₁ and these indices before 1850s. However, it is also true, that 1850s represent the end of Little Ice Age (LIA) period, when ENSO properties and its teleconnections changed significantly. Modeling studies (e.g., Henke et al., 2017) report an increased frequency of El Niño during LIA due to southern displacement of ITCZ. Although the reviewer hypothesis could be true, also our interpretation that decreasing in the correlation between our PC₁ and reconstructed ENSO indices is due to changes in ENSO teleconnections over Europe could be true.

We agree with the reviewer that a comparison with ENSO reconstruction which are trained within the last 150 years can be problematic, since every reconstruction has its own uncertainties and limits. Confident statements are only possible for the time from 1850 onwards, since instrumental measurements of different climate variables are available. However, the usage of climate reconstructions is the only possibility to test and analyze the teleconnection before 1850 because no observational data is available. Overall, we tested the relationship with three different reconstructions for two different time ranges, where the sample density of isotope network is relatively high and the correlation is getting weaker over time (Li et al., 2011; Li et al., 2013; Dätwyler et al., 2019) which is shown in Table 1. Not only the correlation between the first component of the $\delta^{18}\text{O}_{\text{cel}}$ network and the ENSO reconstructions is getting weaker, also the correlation between different ENSO reconstructions is getting weaker in the 18th century which was shown for specific periods in Dätwyler et al. (2019). They suggest that is based on changes of the ENSO teleconnections, because they found a consistent teleconnection pattern that is different to the known teleconnection pattern of ENSO in the instrumental period (Dätwyler et al., 2019).

	LI ET AL. 2011	LI ET AL. 2013	DÄTWYLER ET AL. 2019
1750-1849	r=0.121 p-value=0.231	r=-0.008 p-value=0.936	r=-0.078 p-value=0.442
1850-1949	r=0.223 p-value=0.026	r=0.303 p-value=0.002	r=0.296 p-value=0.003

Table 1: Correlation between the first component of the $\delta^{18}\text{O}_{\text{cel}}$ network with three different ENSO reconstructions for two different time periods.

In order to show how stable the connection between the sea surface temperature (SST) of the tropics and the first mode of $\delta^{18}\text{O}_{\text{cel}}$ is, we have computed stability maps of the correlation between these two quantities. The stability map is a tool which is primarily used for streamflow predictions to identify stable teleconnection (for more details see Ionita et al. (2008), Lohmann et al. (2005) or Rimbu et al. (2005)). SST anomalies from the Extended Reconstructed Sea Surface Temperature (ERSST) v5 dataset (Huang et al., 2017) have been correlated with the first mode of $\delta^{18}\text{O}_{\text{cel}}$ in a moving window of 21 years. The correlation is considered to be stable for those grid points where anomalies are significantly correlated at the 90% level ($r = 0.25$) for more than 80% of the 21-yr windows, covering the period 1850–2005. This is shown in Figure 1. The results from the stability maps analysis will be also integrated in the revised version of the manuscript.

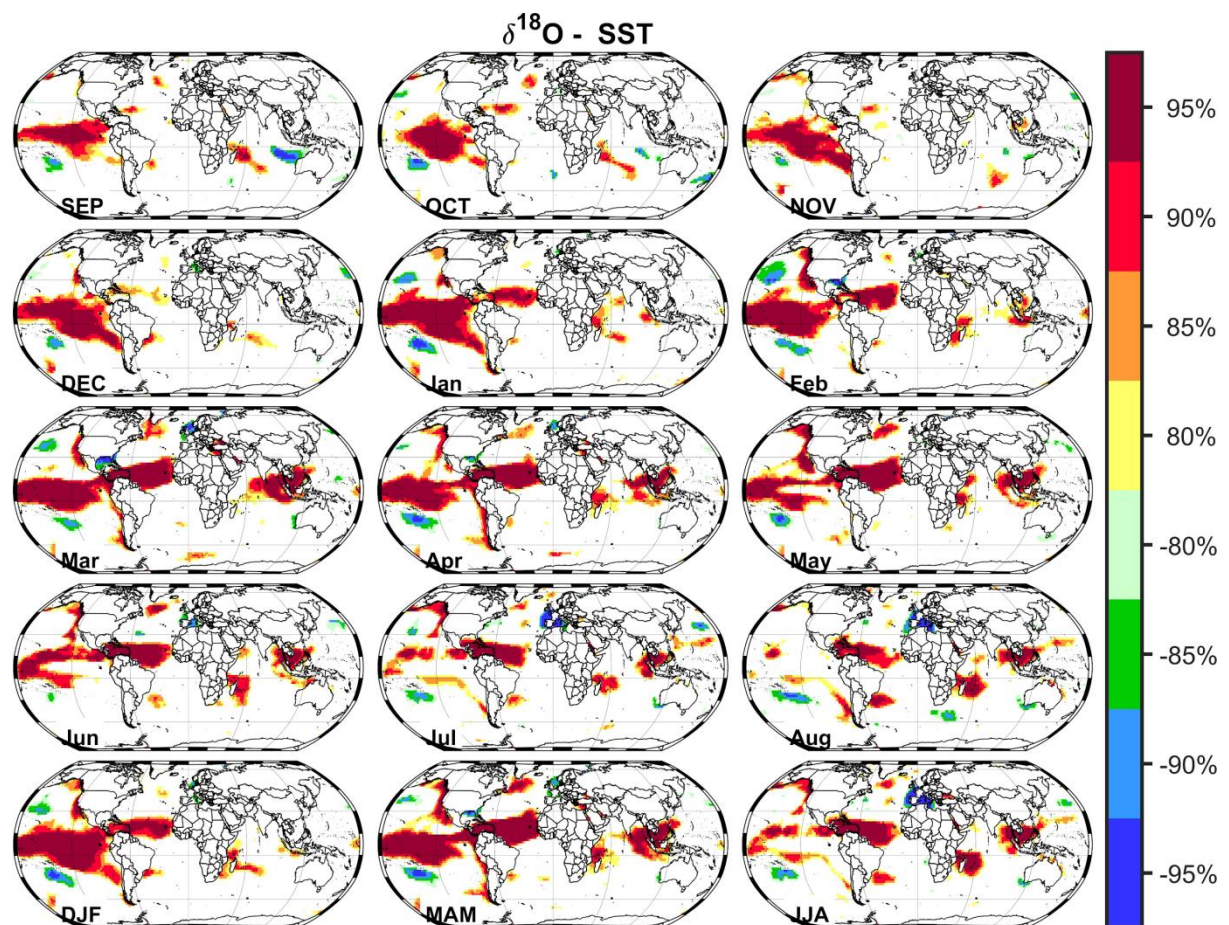


Figure 1: Stability maps for the correlation between SST anomalies (Huang et al., 2017) and the first mode of $\delta^{18}\text{O}_{\text{cel}}$. The color bar indicates how many years are characterized by a significant correlation (at the 90% level) in a 21-yr window, covering the period 1850–2005. Positive correlations are shown from yellowish to reddish and negative correlations from greenish to blueish.

As it can be inferred from Figure 1 (below), one of the largest locations with stable correlations is located in the tropical Pacific. Stable correlations are shown from September (last year) to June which also supports our result that $\delta^{18}\text{O}_{\text{cel}}$ is able to capture a multi-seasonal signal and that the first mode of $\delta^{18}\text{O}_{\text{cel}}$ is sensitive for ENSO variability. With the help of these maps, it is also possible to track the development of the correlation over time. During July and August, the pattern dissolves in the tropical Pacific whereas a stable negative correlation is shown around Europe. Based on these results, we suggest that the relation between the first mode of $\delta^{18}\text{O}_{\text{cel}}$ and the SST in the tropical Pacific/Atlantic in winter and spring is stable in the period from 1850 to 2005.

Based on the suggestions and critical comments of reviewer #2, we have added a subsection to discuss the stability of the link to ENSO variability [subsection 4.3]. Furthermore, we have highlighted the comparison to other ENSO reconstructions and uncertainties especially given by ENSO reconstructions in the new subsection of the revised manuscript.

Furthermore, we have checked carefully the usage of the term “non-stationarity” in the revised manuscript. We also tried to highlight that we can only suggest that the relationship between ENSO and the European climate may be not stable over time. Finally, we would like to thank reviewer #2 for the critical evaluation.

2. The conclusion that the analysis shows that “We infer that the investigation of large-scale atmospheric circulation patterns and related teleconnections far beyond instrumental records can be done with oxygen isotopic signature derived from tree rings.” is not convincingly demonstrated. There is only 2 line in the introduction which gives a hint why this should be possible, i.e., fractionation happens during the transport from source to sink areas. Most of the studies however try to reconstruct temperature and precipitation when using $\delta^{18}\text{O}$ as $\delta^{18}\text{O}$ is first order temperature dependent. The authors also nicely discuss that fractionation processes are also relevant within the tree. Then, at the different sites the water can be transported from different source regions during the seasonal cycle, e.g., North Atlantic versus Mediterranean, or long-distance transport versus local water recycling. Moreover, seasonality plays an important role, so mostly tree ring records are interpreted to record growing season signals and not winter signals. So, given all these uncertainties how can the transport aspect (which is related to the atmospheric circulation) survive?

R: We agree with the reviewer that transport can lead to uncertainties. The earth system is interconnected and includes many factors that make it hard to identify a single cause. Nevertheless, we think that the aforementioned statement of the reviewer is somehow mixes up several points. First of all, the source of oxygen isotopes in cellulose is mostly the water from the atmosphere. Through precipitation, the soil gets enriched with water and

depending on the length and depth of the root system, a tree uses surface water or water from groundwater reservoirs for photosynthesis processes. Therefore, $\delta^{18}\text{O}_{\text{cel}}$ is coupled to the hydrological cycle on Earth. This cycle is strongly dependent on large-scale atmospheric circulation, since large-scale flows determine the path of clouds, precipitation patterns and the distribution of water vapor in the atmosphere. Also, the mentioned water transport from different source regions is related to large-scale atmospheric circulation. Synoptic patterns and associated indices (e.g., cyclone and anticyclone activity, air pressure) have also been reconstructed from $\delta^{18}\text{O}_{\text{cel}}$, with stronger correlations revealed during extreme years or periods (e.g., Saurer et al., 2012). $\delta^{18}\text{O}_{\text{cel}}$ is related to the $\delta^{18}\text{O}$ of the precipitation source via soil water. $\delta^{18}\text{O}$ of soil water constitutes the $\delta^{18}\text{O}$ input to the arboreal system and represents an average $\delta^{18}\text{O}$ over several precipitation events modified by partial evaporation from the soil (depending on soil texture and porosity) and by a possible time lag, depending on rooting depth (Saurer et al., 2012). $\delta^{18}\text{O}_{\text{cel}}$ is further dependent on two tree-internal processes: evaporative ^{18}O -enrichment of leaf or needle water via transpiration, as well as biochemical fractionations and isotopic exchange of $\delta^{18}\text{O}$ with trunk water during cellulose biosynthesis (e.g., Barbour, 2007; Kahmen et al., 2011; Roden et al., 2000; Saurer et al., 2012; Treydte et al., 2014). Fractionations occurring at leaf level, are partly reset by isotopic exchange between sugar oxygen and stem water during cellulose synthesis in the trunk allowing the soil water isotopic signal to be largely preserved in the tree-ring cellulose (e.g., Gessler et al., 2014 and citations therein).

The seasonality is essential since trees store the climate signal within the $\delta^{18}\text{O}_{\text{cel}}$ ratio during the growing season. One of the key messages of the manuscript is that winter climate signals can be stored which is shown by significant correlation plots [Figure 7]. We argue that this is possible through hydrological feedback processes (e.g., via the soil moisture content). The fact that trees are able to store a winter signal is not new and was published for example by Treydte et al. (2006) and Treydte et al. (2014).

With the knowledge about the physical climate processes (the hydrological cycle) and the understanding of the theory behind the fractionation of $\delta^{18}\text{O}_{\text{cel}}$ ratio, we feel that the points mentioned by the reviewer are not uncertainties. They are part of the climate system and essential for the understanding of climate proxies.

We thank the reviewer for the critical comment, which gave us some hints for the discussion of the $\delta^{18}\text{O}_{\text{cel}}$ climate signal [subsection 4.4 & 4.5].

3. For the first EOF I have a different interpretation, which takes into account the fact that temperature play the dominant role in $\delta^{18}\text{O}$. What we see is a monopole structure. The authors claim to see a link to ENSO. I hypothesize that the link is simply due to the fact that

ENSO has a global impact on the global mean temperature. So, due to an El Niño event, the Earth warms and thus also the North Atlantic and the Mediterranean (visible in the composite plots). Warmer source regions affect the fractionation of $\delta^{18}\text{O}$ without any change of the circulation we see in the sink regions (at the tree sites) a uniform signal.

R: The climate over the European region has a rather peculiar variability, and in most of the cases the first EOF is monopolar, especially if we consider mostly the central and western part of Europe in the analysis (like in our isotope network). This is valid for precipitation, temperature and even for drought indices. As we discussed in the first point raised by the reviewer, we disagree that the relationship with ENSO is purely by chance given the tests of statistical significance. The fact that PC1 correlates significantly with the SST from the tropical Pacific in winter and this signal is transmitted to the tropical Atlantic in spring and central Atlantic in summer is part of the natural cycle of ENSO. The ENSO anomalies (either El Niño or La Niña) develop in winter and it needs 3-6 months to see a signal in the European climate. This lagged relationship is typical for many ENSO related teleconnections. This long transition from the tropical Pacific to central North Atlantic affects in turn the large-scale atmospheric circulation and as a consequence the climate over Europe, especially in spring and summer. We do not agree with the idea that just because we have El Niño or La Niña the earth will be either warm or colder. ENSO dynamics are more complicated than this and the signal from ENSO to the $\delta^{18}\text{O}$ is transmitted mainly via the large-scale atmospheric circulation.

In the composite maps, the ENSO teleconnection patterns are clearly emphasized. This means that there is not only a thermodynamical influence on $\delta^{18}\text{O}$, that is variation of global temperature with ENSO, playing a role, but also ENSO related teleconnections impact on European climate is important.

4. There are problems with the data (see comment below Section 2.2, L132-140, L145) ignored which might be influential to the analysis.

R: In the revised version of the manuscript, we have sustainably changed the data section [subsection 2.1 - 2.3]. We have implemented a better description of the used isotope network and a detailed description of the climate data. Please see our detailed answers and argumentation to the aforementioned comment below.

Minor comments

L18: What is meant by "reflects a multi-seasonal climatic signal."? ENSO works on timescales of 3 to 7 years.

R: Quote from the submitted manuscript (L17-18): "The first mode of $\delta^{18}\text{O}$ variability is associated with anomaly patterns of the El Niño-Southern Oscillation (ENSO) and reflects a multi-seasonal climatic signal". So, the last part of the sentence is connected to the first mode of $\delta^{18}\text{O}$ which means that the first mode of $\delta^{18}\text{O}$ variability reflects a multi-seasonal climatic signal. The multi-seasonal climatic signal stored in $\delta^{18}\text{O}$ is essential to capture El Niño/La Niña events and the related ENSO variability.

L20: "out of phase variability": I would interpret this in the time and not in space as the authors. Just say the 2. EOF is a dipole pattern with centers over northwestern and southeastern Europe.

R: Thank you for the suggestion. We have rewritten it in the revised version of the manuscript [L20].

L47-50: Hard to read.

R: We have revised the mentioned section [L45-48].

L53: please change to "leaf water clearly affects"

R: We have changed the sentence according to the suggestion of the reviewer [L50].

L55: I disagree with this statement, see major comments 2 and 3.

R: In this point, we disagree with the reviewer. Please have a look above for our argumentation.

L56: What is meant by "resulting long-term perspective"? Where does it result from?

R: Thanks to the reviewer for highlighting this. We mean the long-term perspective that results from the usage of $\delta^{18}\text{O}_{\text{cel}}$ as a climate proxy. We have rewritten the sentence to make it clearer [L54-56].

L84: Created -> generated

R: We have changed it [L81].

L88: Please include a space between number and unit throughout the manuscript.

R: We have improved it in the revised version of the manuscript [L86].

L91: What is SMOW?

R: It should be VSMOW (Vienna Standard Mean Ocean Water). We have changed it [L89].

Section 2.1: Which method is used to get the delta18O samples from trees. This is relevant as studies show that the method (pooling or not pooling) makes a huge difference Hangartner et al. Methods to merge overlapping tree-ring isotope series to generate multi-centennial chronologies CHEMICAL GEOLOGY Volume: 294 Pages: 127-134 Published: FEB 10 2012

R: We agree with the reviewer that information about the sampling method is very important. According to Treydte et. al (2007a, b), all tree rings from the same year were pooled prior to cellulose extraction for the majority of sites. We have added this in Section 2.1 in the revised version of the manuscript [L92-93].

Section 2.2: Again it is unclear what the authors are using. Is it the ensemble mean of 20CR or an individual ensemble member. Please note that the 20CR is only constrained with sea level pressure (SLP) data so no sea surface temperatures (SST) are used which are relevant for ENSO. My guess is that the authors use the ensemble mean. This is problematic as in the early part of the reanalysis the constraint (via SLP) is rather weak leading to variance deflation and thus can have a strong impact on the analysis (so it is normally recommended to use all individual ensemble members). As said, the other problem is that ENSO might not be realistically included in the first part of the reanalysis.

R: The argumentation that 20CR (V2c) is not using SST is not correct since the SST dataset from 18 members of Simple Ocean Data Assimilation with Sparse Input version 2 (SODAsi.2, Giese et al., 2016) are used as SST boundary condition (the high latitudes (>60°) were corrected to COBE-SST2 (Hirahara et al. 2014)). Furthermore, the sea ice cover (SIC) reconstruction of Hirahara et al. (2014) is also used as boundary condition (for more details see https://www.psl.noaa.gov/data/gridded/data.20thC_ReanV2c.html). Therefore, the SST and SIC are influencing the atmosphere (Compo et al, 2011) and therefore, ENSO activity is represented in 20CR (V2c).

Nevertheless, we have tried to explain the used climate data more in detail in the revised version of the manuscript. For this purpose, most of the climate data subsection have been rewritten. Additionally, we have added climate data from other sources to get more confidence for our results and to convince reviewer #2 of the correctness of our results [subsection 2.2].

Section 2.3: too short and not clear why the simulations are used and how the simulations are generated. The reader needs to understand which model is used and how, just references is not enough.

R: We thank the reviewer for pointing out that the subsection a 'nudged model scenarios/simulation' was not well explained and also confusing. The subsection has been renamed and sustainably changed with a better explanation of the technique behind and an argumentation why we used the model output [subsection 3.3].

Section 2.4: It reads like EOF and PCA are different analysis, but actually they are not. The method of empirical orthogonal function (EOF) analysis is a decomposition of a data set in terms of orthogonal basis functions determined from this data. Thus it is the same as geographically weighted PCAs.

Overall, the PCA and EOF technique are related, but differences exist and both abbreviations are often mixed up. For detailed explanation of the differences, we refer to our response to reviewer #1 (L123-131). Based on the comments of both reviewers, we have rewritten our explanation of the PCA and EOF technique. Furthermore, we have added a more detailed explanation of the North et al. (1982) rule [L153-170].

L132-140: How many tree ring records cover the entire period with no gaps? How sensitive is the analysis to filling the gaps? How many cycles are needed to reach convergence? What if you use only the tree ring records which cover the entire period?

R: Twelve time series cover the entire period. Since, our goal is to use all time series of the ISONET+ product and therefore, we have to fill the gaps. If we calculate the EOFs and PCs for the period 1850 to 1998 the spatial and temporal correlation to the EOFs and PCs for the entire period is very high. If we remove samples in the period 1850 to 1998, also the PCs and EOFs are changing because the input variability of the network is changing. The results are similar patterns, but the temporal and spatial correlation is varying. For a comparison of the climate signal of the used $\delta^{18}\text{O}_{\text{cel}}$ network, the reader is referred to the publication of the used isotope network of Treydte et al (2007b). Based on the comments of both reviewers, we have added a new section in the methods [179-183] and in the results [L244-L254] which contextualizes the used gap filling method and the uncertainties. Furthermore, we have added a table in the supplement to describe the characteristics of each time series and sample site [Supp. 1].

L142: This is certainly not extreme.

R: The detection of extremes by using the standard deviation is often used in climate science. There are many other definitions of extremes. We decided to use the standard deviation as an approximation given the available degrees of freedom. These extremes may not be extremely rare but certainly unusual and different from the mean.

L145: I would say that the authors misuse the composite analysis by focusing on the linear response. If they would like to analyze the linear response, a simple correlation analysis is enough. The beauty of the composite analysis is that you can easily show non-linear effects, but only if you make the difference between the mean above the threshold with the long term mean and in a second plot the mean below the negative threshold and the long term mean. This was done by Fraedrich 1992 mentioned in the manuscript. He highlighted the nonlinearity of the ENSO response over Europe and thus is in contradiction to the linear relationship suggested here.

R: We think that this point is a misunderstanding of our idea because we used the composite maps to learn more about the linear response. It is not our aim to test relation for non-linearities. The reference of Fraedrich (1992) is used to highlight the uncertainties and show the reader that the shown relationship in the results cannot be seen as linear. In the revised version of the manuscript, we have replaced the figures with new figures in which we show both the high ($PC_1 > 1$ standard deviation) and low ($PC_1 < -1$ standard deviation) composite maps for SST and Z500 [Fig. 4 & 5]. There are cases in which the high and low composite maps show different results, thus indicating non-linearity between the variables analyzed, but in our case the high and low composite maps are similar (in terms of structure), that is why we had shown just the difference map.

L150: Event Coincidence Analysis needs to be explained.

R: Thank you for the comment. We have extended the explanation of the method [L192-199].

L177-179: If this is the case one could speculate that EOF2 showing a North South patterns just resemble this latitudinal effect.

R: In this comment, two essentials were mixed up. First of all, the latitudinal effect was found by Daansgard (1964) and is defined as a steady shift of the isotope values from the equator to the poles. The reason for this is that temperature changes within different seasons and varies over the latitudes. According to Daansgard (1964) and Gat (2010), the mean annual temperature and the $\delta^{18}O$ in the atmosphere are strongly correlated. For a documentation of several effects on the $\delta^{18}O$ ratio, e.g., the continental effect, we refer to the publication of Gat (2010).

The latitudinal effect is important for the $\delta^{18}\text{O}_{\text{cel}}$ ratio at each site (Figure 1 of the submitted manuscript), because it is one factor which influences the source values ($\delta^{18}\text{O}_{\text{precipitation}}$, $\delta^{18}\text{O}_{\text{soilwater}}$). In contrast, the latitudinal effect cannot explain the (climate) variability which is investigated and represented by the PCA and EOF technique in our study. The climate variability is determined by several other quantities which cannot be explained by a simple latitudinal position, e.g., large-scale atmospheric flows. Based on that argumentation, we disagree with the speculation of the reviewer.

L195: I do not see this is there a typo and the authors mean PC1?

R: Thank you for the comment. We have revised the sentence [L243-244].

L200-210: Avoid using the bracket with e.g. (cold). This makes the text unreadable. Just say what you show in Fig. 4.

R: This is the standard way how composite maps are described. It is necessary to add the brackets since both tails of the distribution function are combined and represented in these maps. Therefore, we have to write this additional information to clearly represent both extremes. To make it more understandable, we have added a more detailed explanation of how composite maps are working [L184-190].

L208: I do not see a AO pattern, again the reference to Fraedrich are incorrect as they claim that ENSO has a nonlinear response behavior over Europe.

R: We thank the reviewer for this comment. It is true that there is some asymmetry between El Niño and La Niña teleconnection patterns over Europe. However, the analysis of long-term data reveals that El Niño (La Niña) conditions in the tropical Pacific are associated with a negative (positive) phase of the North Atlantic Oscillation in the North Atlantic region during winter. The composite pattern represented in the figure reflects this ENSO-NAO relationship, although the pattern is not identical with the AO/NAO. In the revised version, we have written more carefully about the similarities to the NAO pattern [L345-351] and have removed the comparison to the AO pattern.

L225: Why drought we see a positive precipitation anomaly?

R: We think that your comment is a misunderstanding of our composite map. As mentioned above both extremes of the distribution are represented by the composite map. We have added a more detailed description of the composite maps for a better understanding [L184-190].

Section 3.4: What do we learn from this? What is shown and why? This section is unclear and to my feeling can be removed.

R: Our goal with the model output is to test the correlation between $\delta^{18}\text{O}_{\text{cel}}$ and $\delta^{18}\text{O}_P/\delta^{18}\text{O}_{\text{SW}}$ to identify if the water, which is used during the photosynthesis processes, has a multi-seasonal isotopic signature. We agree with the reviewer that it is not clearly explained in the manuscript. Therefore, we have added an extended explanation of the used dataset [subsection 2.3] and the results in the revised version of the manuscript [subsection 3.4]. Furthermore, we have added a subsection to discuss the winter climate signal in $\delta^{18}\text{O}_{\text{cel}}$ [subsection 4.4].

L250: section 3.5

R: We have corrected it in the revised version of the manuscript [L307].

L251-252: This sentence is a repetition.

R: We have removed the sentence in the revised version of the manuscript.

L260 -263: You need to show this with more proxies. Note that dry conditions are not droughts!

R: Thank you for the comment. We have been very sensitive with the usage of the term “drought” in the revised version of the manuscript. Furthermore, the comparison with more proxies is a really good idea. Based on the complexity of this topic, this would be another big study and a topic for the future work in this field. In our study, we want to show primarily the results of the analysis of the $\delta^{18}\text{O}_{\text{cel}}$ isotope network.

L263-265: Given your study you cannot conclude this. The authors study certainly is inadequate to reconstruct blocking so this statement is not supported by the authors analysis.

R: We agree with the reviewer that this part was not well discussed and explained. In the revised version of the manuscript, we have added a new subsection to discuss the relation to summer atmospheric blocking [subsection 4.5].

L269-70: Please change to “. . . signal still dominates”.

R: We have rewritten it [L437].

Figures: Statistical significance is not tested (or not shown).

R: In the revised version of the manuscript, we have replaced the former figures with figures which are also showing the significance [Fig. 4,5,6,8 & 9].

References used in our responses to both anonymous referees:

- Álvarez, C., Veblen, T. T., Christie, D. and González-Reyes, Á.: Relationships between climate variability and radial growth of *Nothofagus pumilio* near altitudinal treeline in the Andes of northern Patagonia, Chile, , doi:10.1016/J.FORECO.2015.01.018, 2015.
- Barbour, M. M.: Stable oxygen isotope composition of plant tissue: a review, *Funct Plant Biol*, 34, 83–94, 2007.
- Butzin, M., Werner, M., Masson-Delmotte, V., Risi, C., Frankenberg, C., Gribanov, K., Jouzel, J. and Zakharov, V. I.: Variations of oxygen-18 in West Siberian precipitation during the last 50 years, *Atmospheric Chemistry and Physics*, 14(11), 5853–5869, doi:[10.5194/acp-14-5853-2014](https://doi.org/10.5194/acp-14-5853-2014), 2014.
- Brönnimann, S., Xoplaki, E., Casty, C., Pauling, A. and Luterbacher, J.: ENSO influence on Europe during the last centuries, *Climate Dynamics*, 28(2–3), 181–197, doi:10.1007/s00382-006-0175-z, 2007.
- Compo, G. P., Whitaker, J. S., Sardeshmukh, P. D., Matsui, N., Allan, R. J., Yin, X., Gleason, B. E., Vose, R. S., Rutledge, G., Bessemoulin, P., Brönnimann, S., Brunet, M., Crouthamel, R. I., Grant, A. N., Groisman, P. Y., Jones, P. D., Kruk, M. C., Kruger, A. C., Marshall, G. J., Maugeri, M., Mok, H. Y., Nordli, Ø., Ross, T. F., Trigo, R. M., Wang, X. L., Woodruff, S. D. and Worley, S. J.: The Twentieth Century Reanalysis Project, *Quarterly Journal of the Royal Meteorological Society*, 137(654), 1–28, doi:10.1002/qj.776, 2011.
- Dansgaard, W.: Stable isotopes in precipitation, *Tellus*, 16(4), 436–468, doi:10.1111/j.2153-3490.1964.tb00181.x, 1964.
- Dätwyler, C., Abram, N. J., Grosjean, M., Wahl, E. R. and Neukom, R.: El Niño–Southern Oscillation variability, teleconnection changes and responses to large volcanic eruptions since AD 1000, *International Journal of Climatology*, 39(5), 2711–2724, doi:10.1002/joc.5983, 2019.
- Deser, C., Capotondi, A., Saravanan, R. and Phillips, A. S.: Tropical Pacific and Atlantic Climate Variability in CCSM3, , doi:10.1175/JCLI3759.1, 2006.
- Fraedrich, K.: An ENSO impact on Europe?, *Tellus A*, 46(4), 541–552, doi:10.1034/j.1600-0870.1994.00015.x, 1994.
- Fraedrich, K. and Müller, K.: Climate anomalies in Europe associated with ENSO extremes, *International Journal of Climatology*, 12(1), 25–31, doi:10.1002/joc.3370120104, 1992.
- Gat, J.: *Isotope Hydrology: A Study of the Water Cycle*, World Scientific, London., 2010.
- Gessler, A., Ferrio, J. P., Hommel, R., Treydte, K., Werner, R. A., and Monson, R. K.: Stable isotopes in tree rings: towards a mechanistic understanding of isotope fractionation and mixing processes from the leaves to the wood, *Tree Physiology*, 34, 796–818, 2014.
- Henke LMK 2017, Was Little Ice Age more or less El Nino like than Medieval Climate anomaly? *Climate of the past*, doi: 10.5194/cp-13-267-2017
- Hirahara, S., Ishii, M. and Fukuda, Y.: Centennial-Scale Sea Surface Temperature Analysis and Its Uncertainty, *Journal of Climate*, 27(1), 57–75, doi:10.1175/JCLI-D-12-00837.1, 2014.
- Hotelling, H.: The most predictable criterion, *Journal of Educational Psychology*, 26(2), 139–142, doi:10.1037/h0058165, 1935.
- Huang, B., Thorne, P. W., Banzon, V. F., Boyer, T., Chepurin, G., Lawrimore, J. H., Menne, M. J., Smith, T. M., Vose, R. S. and Zhang, H.-M.: NOAA Extended Reconstructed Sea Surface Temperature (ERSST), Version 5, doi:10.7289/V5T72FNM, 2017.
- Ionita, M., Lohmann, G. and Rimbu, N.: Prediction of Spring Elbe Discharge Based on Stable Teleconnections with Winter Global Temperature and Precipitation, *J. Climate*, 21(23), 6215–6226, doi:10.1175/2008JCLI2248.1, 2008.

- Josse, J. and Husson, F.: missMDA : A Package for Handling Missing Values in Multivariate Data Analysis, *Journal of Statistical Software*, 70(1), doi:[10.18637/jss.v070.i01](https://doi.org/10.18637/jss.v070.i01), 2016.
- Kahmen, A., Sachse, D., Arndt, S. K., Tu, K. P., Farrington, H., Vitousek, P. M., and Dawson, T. E.: Cellulose delta O-18 is an index of leaf-to-air vapor pressure difference (VPD) in tropical plants, *Proceedings of the National Academy of Sciences of the United States of America*, 108, 1981-1986, 2011.
- Li, J., Xie, S.-P., Cook, E. R., Huang, G., D'Arrigo, R., Liu, F., Ma, J. and Zheng, X.-T.: Interdecadal modulation of El Niño amplitude during the past millennium, *Nature Climate Change*, 1(2), 114–118, doi:[10.1038/nclimate1086](https://doi.org/10.1038/nclimate1086), 2011.
- Li, J., Xie, S.-P., Cook, E. R., Morales, M. S., Christie, D. A., Johnson, N. C., Chen, F., D'Arrigo, R., Fowler, A. M., Gou, X. and Fang, K.: El Niño modulations over the past seven centuries, *Nature Climate Change*, 3(9), 822–826, doi:[10.1038/nclimate1936](https://doi.org/10.1038/nclimate1936), 2013.
- Lohmann, G., Rimbu, N. and Dima, M.: Where can the Arctic oscillation be reconstructed? Towards a reconstruction of climate modes based on stable teleconnections, *Climate of the Past Discussions*, 1(1), 17–56, 2005.
- Lorenz, E. N.: Prospects for statistical weather forecasting: final report: Statistical Forecasting Project, Massachusetts Institute of Technology, Dept. of Meteorology, Cambridge, Mass. [online] Available from: <https://catalog.hathitrust.org/Record/007185933> (Accessed 16 November 2018), 1959.
- North, G. R., Bell, T. L., Cahalan, R. F. and Moeng, F. J.: Sampling Errors in the Estimation of Empirical Orthogonal Functions, *Mon. Wea. Rev.*, 110(7), 699–706, doi:[10.1175/1520-0493\(1982\)110<0699:SEITEO>2.0.CO;2](https://doi.org/10.1175/1520-0493(1982)110<0699:SEITEO>2.0.CO;2), 1982.
- Pearson, K.: On lines and planes of closest fit to systems of points in space, *The London, Edinburgh, and Dublin Philosophical Magazine and Journal of Science*, 2(11), 559–572, doi:[10.1080/14786440109462720](https://doi.org/10.1080/14786440109462720), 1902.
- Pozo-Vázquez, D., Gámiz-Fortis, S. R., Tovar-Pescador, J., Esteban-Parra, M. J. and Castro-Díez, Y.: El Niño–southern oscillation events and associated European winter precipitation anomalies, *International Journal of Climatology*, 25(1), 17–31, doi:[10.1002/joc.1097](https://doi.org/10.1002/joc.1097), 2005.
- Raible, C. C., Luksch, U. and Fraedrich, K.: Precipitation and Northern Hemisphere regimes, *Atmospheric Science Letters*, 5, 43–55, doi:[10.1016/j.atmoscilet.2003.12.001](https://doi.org/10.1016/j.atmoscilet.2003.12.001), 2004.
- Rimbu, N., Lohmann, G., Felis, T. and Tzold, J. P.: Shift in ENSO Teleconnections Recorded by a Northern Red Sea Coral, *JOURNAL OF CLIMATE*, 16, 9, 2003.
- Rimbu, N., Dima, M., Lohmann, G. and Musat, I.: Seasonal prediction of Danube flow variability based on stable teleconnection with sea surface temperature, *Geophysical Research Letters*, 32(21), doi:[10.1029/2005GL024241](https://doi.org/10.1029/2005GL024241), 2005.
- Roden, J. S., Lin, G. G., and Ehleringer, J. R.: A mechanistic model for interpretation of hydrogen and oxygen isotope ratios in tree-ring cellulose, *Geochimica et Cosmochimica Acta*, 64, 21-35, 2000.
- Saurer, M., Kress, A., Leuenberger, M., Rinne, K. T., Treydte, K. S., and Siegwolf, R. T. W.: Influence of atmospheric circulation patterns on the oxygen isotope ratio of tree rings in the Alpine region, *Journal of Geophysical Research-Atmospheres*, 117, 2012.
- Schönwiese, C.-D.: *Praktische Statistik für Meteorologen und Geowissenschaftler*, Borntraeger, Berlin., 2013.
- Storch, H. v and Zwiers, F. W.: *Statistical analysis in climate research*, Cambridge University Press, Cambridge ; New York., 1999.
- Treydte, K., Schleser, G. H., Helle, G., Frank, D. C., Winiger, M., Haug, G. H. and Esper, J.: The twentieth century was the wettest period in northern Pakistan over the past millennium, *Nature*, 440(7088), 1179–1182, doi:[10.1038/nature04743](https://doi.org/10.1038/nature04743), 2006.

Treydte, K., Schleser, G. H., Esper, J., Andreu, L., Bednarz, Z. and Berninger, F.: Climate signals in the European isotope network ISONET, TRACE, 5, 138–147, 2007a.

Treydte, K., Frank, D., Esper, J., Andreu, L., Bednarz, Z., Berninger, F., Boettger, T., D'Alessandro, C. M., Etien, N., Filot, M., Grabner, M., Guillemin, M. T., Gutierrez, E., Haupt, M., Helle, G., Hilarvuori, E., Jungner, H., Kalela-Brundin, M., Krapiec, M., Leuenberger, M., Loader, N. J., Masson-Delmotte, V., Pazdur, A., Pawelczyk, S., Pierre, M., Planells, O., Pukiene, R., Reynolds-Henne, C. E., Rinne, K. T., Saracino, A., Saurer, M., Sonninen, E., Stievenard, M., Switsur, V. R., Szczepanek, M., Szychowska-Krapiec, E., Todaro, L., Waterhouse, J. S., Weigl, M. and Schleser, G. H.: Signal strength and climate calibration of a European tree-ring isotope network, Geophysical Research Letters, 34(24), doi:10.1029/2007GL031106, 2007b.

Treydte, K., Boda, S., Graf Pannatier, E., Fonti, P., Frank, D., Ullrich, B., Saurer, M., Siegwolf, R., Battipaglia, G., Werner, W., and Gessler, A.: Seasonal transfer of oxygen isotopes from precipitation and soil to the tree ring: source water versus needle water enrichment, New Phytol, 202, 772-783, 2014.

Large-scale climate signals of a European oxygen isotope network from tree-rings

Daniel F. Balting¹, Monica Ionita¹, Martin Wegmann¹, Gerhard Helle², Gerhard H. Schleser³, Norel Rimbu¹, Mandy B. Freund^{4,5}, Ingo Heinrich^{2,6}, Diana Caldarescu¹ & Gerrit Lohmann^{1,7}

5 ¹Alfred Wegener Institute, Bremerhaven, 27570, Germany

²German Research Centre for Geosciences, Potsdam, 14473, Germany

³IBG-3, Forschungszentrum Jülich, 52428, Germany

⁴Climate and Energy College, University of Melbourne, Melbourne, 3010, Australia

⁵CSIRO Agriculture and Food, Melbourne, Australia

10 ⁶Geography Department, Humboldt University, Berlin, 10099, Germany

⁷Physics Department, University of Bremen, Bremen, 28359, Germany

Correspondence to: Daniel F. Balting (daniel.balting@awi.de)

15 **Abstract.** We investigate the **climate signature** of $\delta^{18}\text{O}$ tree ring records from sites distributed all over Europe covering the last 400 years. An Empirical Orthogonal Function (EOF) analysis reveals two distinct modes of variability on the basis of the existing $\delta^{18}\text{O}$ tree ring records. The first mode is associated with anomaly patterns **projecting onto** the El Niño-Southern Oscillation (ENSO) and reflects a multi-seasonal climatic signal. The ENSO **link is pronounced** for the last 130 years, but is found **to be weak over** the period 1600 to 1850, suggesting that the relationship between ENSO and the European climate
20 may not **be stable** over time. The second mode of $\delta^{18}\text{O}$ variability, which captures **a north-south dipole in the** European $\delta^{18}\text{O}$ tree ring records, is related to a regional summer atmospheric circulation pattern revealing a pronounced centre over the North Sea. Locally, the $\delta^{18}\text{O}$ anomalies associated with this mode show the same (opposite) sign with temperature (precipitation). **Based on the oxygen isotopic signature derived from tree rings, we argue** that the **prevailing** large-scale atmospheric circulation patterns and **the** related teleconnections **can be analyzed** beyond instrumental records.

25

1 Introduction

Tree growth is irrevocably affected by interactions with hydrosphere, atmosphere, and pedosphere and the influence of environmental factors is stored in the physical and chemical properties of each tree ring (Schweingruber, 1996). A major component of a tree ring is cellulose, which consists of the elements carbon, oxygen and hydrogen. Their stable isotope
30 signatures are determined by varying environmental conditions influencing a series of fractionation processes during the uptake of CO_2 and H_2O from atmosphere and soil and biosynthesis of tree-ring cellulose. For instance, the climate signature of $\delta^{13}\text{C}$ values of tree-ring cellulose basically originates from fractionations during photosynthesis at the leaf or needle level that generally lower the $\delta^{13}\text{C}$ of the atmospheric CO_2 source which contains no direct climatic signal (e.g. Schleser et al., 1995). $\delta^{18}\text{O}$ of tree-ring cellulose ($\delta^{18}\text{O}_{\text{cel}}$) is of particular interest for paleoclimate studies because it is related to source
35 water, i.e. $\delta^{18}\text{O}$ of precipitation ($\delta^{18}\text{O}_{\text{p}}$), which is directly affected by climate processes, **such as** temperature during droplet

condensation within air masses, transport distance from ocean source, type of precipitation (e.g. rain or snow) and precipitation amount (e.g. Dansgaard, 1964; Epstein et al., 1977; Rozanski et al., 1993). Within the arboreal system, $\delta^{18}\text{O}$ of soil water ($\delta^{18}\text{O}_{\text{sw}}$) constitutes the $\delta^{18}\text{O}$ input and usually represents an average $\delta^{18}\text{O}_{\text{p}}$ over several precipitation events modified by partial evaporation from the soil (depending on soil texture and porosity) and by a possible time lag, depending on rooting depth (Saurer et al., 2012). Representing the baseline variability, the oxygen isotope signature of tree-ring cellulose ($\delta^{18}\text{O}_{\text{cel}}$) is invariably tied to $\delta^{18}\text{O}_{\text{sw}}$.

However, $\delta^{18}\text{O}_{\text{cel}}$ is dependent on two more clusters of fractionations that reflect tree-internal processes, namely evaporative ^{18}O -enrichment of leaf or needle water via transpiration, and biochemical fractionations including partial isotopic exchange of cellulose precursors with trunk water during cellulose biosynthesis (e.g. Saurer et al., 1997; Roden et al., 2000; Barbour, 2007; Kahmen et al., 2011; Treydte et al., 2014 and citations therein). The biochemical fractionation during cellulose biosynthesis can be largely considered as constant at $27 \pm 4\%$ (Sternberg and DeNiro, 1983). Nonetheless, varying leaf-to-air vapour pressure deficit together with a varying air humidity causes corresponding changes in the $\delta^{18}\text{O}$ signature of leaf or needle water (e.g. Helliker and Griffiths, 2007). Although modified and dampened by physiological processes (e.g. Pèclet effect (Farquhar and Lloyd, 1993)) and oxygen isotope exchange with stem water during cellulose synthesis (Hill et al., 1995) variability of ^{18}O enrichment of leaf-water clearly affects $\delta^{18}\text{O}_{\text{cel}}$, besides the strong signature of $\delta^{18}\text{O}_{\text{p}}$. For example, the $\delta^{18}\text{O}_{\text{cel}}$ are used to reconstruct precipitation (e.g. Rinne et al., 2013), air temperature (e.g. Porter et al., 2014) and drought (e.g. Nagavciuc et al., 2019). Since these quantities are largely based on transport processes within the atmosphere, the $\delta^{18}\text{O}_{\text{cel}}$ values can be used to get detailed information about large-scale atmospheric circulation patterns (Brienen et al., 2012; Lavergne et al., 2016; Andreu-Hayles et al., 2017; Trouet et al., 2018, Nagavciuc et al., 2019). The resulting long-term perspective on the climate from the usage of $\delta^{18}\text{O}_{\text{cel}}$ as a climate proxy may be the key to identify the influence of different external forcing on, and internal variability of the behaviour of large-scale atmospheric circulation.

One of the most important components for the internal climate variability is the El Niño – Southern Oscillation (ENSO) which influences the atmospheric circulation globally (Allan et al., 1996). Since ENSO variability is strongest in winter, multiple studies have identified a significant ENSO impact on the European climate during this season. Observational studies (Fraedrich and Müller, 1992; Fraedrich, 1994; Brönnimann et al., 2004; Pozo-Vazquez et al., 2005; Brönnimann et al., 2007) and model studies (Merkel and Latif, 2002; Mathieu et al., 2004) suggest that an El Niño event leads to a negative phase of the North Atlantic Oscillation (NAO) with cold and dry conditions over Northern Europe and wet and warm conditions over southeaster Europe in winter. Furthermore, it is also possible to identify a significant ENSO influence with regard to European precipitation in spring (van Oldenborgh, 1998; Lloyd-Hughes and Saunders, 2002; Brönnimann et al., 2007; Helama et al., 2009). However, significant impacts of ENSO regarding European droughts could only be detected for the most extreme El Niño events (King et al., 2020). To what extent these preconditions influence the climate conditions during summer is not yet known for Europe, but it can serve as a key for a better understanding of European climate. However, the relatively short period of existing instrumental data (van Oldenburgh and Burgers, 2005; Brönnimann, 2007),

70 makes it difficult to describe the full range of ENSO variability and its possible consequences for the climate of the European continent (Domeisen et al., 2019).

The aim of this study is to present a comprehensive spatio-temporal analysis of the large-scale European atmospheric circulation based on the climatological signals of a European $\delta^{18}\text{O}_{\text{cel}}$ network, extending back for ~400 years. This study is based on the climatological signals of a European $\delta^{18}\text{O}_{\text{cel}}$ network. The climate signal of the isotope network is extracted by using an Empirical Orthogonal Functions (EOF) analysis. The results of the first two components are compared to climate data and different ENSO reconstructions. The comparison is done by a composite analysis and by correlation analysis. To test if $\delta^{18}\text{O}_{\text{cel}}$ can capture multi seasonal signals, the first component of the isotope network is correlated with gridded fields of modelled $\delta^{18}\text{O}_p$ and $\delta^{18}\text{O}_{\text{sw}}$. Finally, the major results are critically discussed and compared to other studies.

2 Data and Methods

2.1 The isotope network

80 In this study, we investigate the first two dominant modes of variability of 26 $\delta^{18}\text{O}_{\text{cel}}$ records, distributed over Europe, and their relationships with regional and large-scale climate anomalies. 22 of the 26 $\delta^{18}\text{O}_{\text{cel}}$ records were generated within the EU project ISONET (Annual Reconstructions of European Climate Variability using a High-Resolution Isotopic network) (Treydte et al., 2007a, b). Furthermore, four additional sites from Bulgaria, Turkey, Southwest Germany and Slovenia were added to the ISONET network for the current study. (Heinrich et al., 2013; Hafner et al., 2014). In total, the isotope network contains eight broadleaf tree sites (*Quercus*) and 18 coniferous tree sites (*Pinus*, *Juniper*, *Larix*, *Cedrus*) from altitudes varying for each location from 10 m up to 2200 m above sea level (Fig. 1 and Supp. 1). 24 of the 26 sites are distributed over the European continent whereas two additional sites are located in the Atlas Mountains of Morocco and in the Taurus Mountains of Turkey.

90 The stable isotopes of oxygen in tree-ring cellulose, reported as $\delta^{18}\text{O}_{\text{cel}}$ vs. Vienna Standard Mean Ocean Water (Craig, 1957) of each site were determined as described by Treydte et al. (2007a, b). At least four dominant trees were chosen per site and two increment cores were taken per tree. After the standard dendrochronological dating following Fritts (1976), the individual tree rings were dissected from the cores. According to Treydte et al. (2007a, b), all tree rings from the same year were pooled prior to cellulose extraction for the majority of sites. However, for oak only the latewood was used for the analyses. This procedure assumed that climate signals of the current year were predominantly applied since early wood of oaks frequently contains climate information of the preceding year. This is based on the fact that the proportion of the reserves of deciduous trees of the isotope network is higher at the beginning of the tree ring formation as in comparison with conifers of the isotope network because they are evergreen. The temporal resolution of the isotope records is annually. The first 100 years of data from the network as well as a general description have already been published (Treydte et al., 2007a, b). Data from individual sites or regional groups of sites were published elsewhere (Saurer et al., 2008; Vitas, 2008;

100 Etien et al., 2009; Hilasvuori et al., 2009; Haupt et al., 2011; Saurer et al., 2012; Rinne et al., 2013; Helama et al., 2014; Labuhn et al., 2014; Saurer et al., 2014; Labuhn, et al., 2016; Andreu-Hayles et al., 2017). Here, we use the extended ISONET+ product where the longest chronologies cover a period from 1600 to 2005. The highest data density is available for the period 1850-1998 with 26 time series available for further analysis. 12 time series cover the entire period of 400 years.

105 2.2 Climate data

For gridded the climate information, we used the gridded fields of monthly temperature averages and monthly precipitation sums from the Climatic Research Unit version 4.04 (Harris et al., 2020). Both quantities are derived by the interpolation of monthly climate anomalies from extensive networks of weather station observations. The CRU TS dataset has a spatial resolution of $0.5^\circ \times 0.5^\circ$ and they cover the period 1901 – 2019.

110 Since precipitation and temperature are both important for the $\delta^{18}\text{O}_{\text{cel}}$ ratio, we want to test the relation between the used isotope ratio and drought conditions. For this purpose, the Standardized Precipitation Evapotranspiration Index dataset from Vicente-Serrano et al. (2010) is used in this study with aggregation time of three months (SPEI3). The SPEI3 index is suitable for this analysis because we want to take into account the climate conditions of the pre-season. Furthermore, the Extended Reconstructed Sea Surface Temperature version 5 (ERSST5; Huang et al., 2017) is included in the study to investigate the correlation between the global sea surface temperature (SST) and the climate signals of $\delta^{18}\text{O}_{\text{cel}}$. 115 The ERSST5 dataset was created by Huang et al. (2017) and it is derived from the International Comprehensive Ocean–Atmosphere Dataset. The monthly SST fields has a spatial resolution of $2^\circ \times 2^\circ$ and they are available for the time range from 1854 to present. The gridded fields of the ERSST5 dataset are provided by NOAA/OAR/ESRL PSL, Boulder, Colorado, USA and they can be downloaded from their website (www1.ncdc.noaa.gov/pub/data/cmb/ersst/v5/netcdf/). All of 120 the mentioned climate data were seasonally averaged: DJF (December to February), MAM (March to May), JJA (June to August) and SON (September to November). Furthermore, the linear trend from each grid cell has been removed. Since our study is focused on the relation between ENSO variability and the $\delta^{18}\text{O}_{\text{cel}}$ network, we used also the anomaly (1981-2010 mean removed) of the December Nino 3.4 index (HadISST1; Rayner et al., 2003). The index represents the averaged SST from 5°S - 5°N and 170° - 120°W (downloadable from https://psl.noaa.gov/gcos_wgsp/Timeseries/Nino34/). To 125 compare the relation between ENSO variability and our Isotope network variability, also in the past, three different reconstruction of ENSO activity have been used in this study: i) the reconstruction of Dätwyler et al. (2019) of the annually Niño3.4 index for the last millennium (based on a multiproxy network); ii) the reconstruction of NDJ Niño3.4 index for the last 700 years by Li et al. (2013) (based on a tree-ring network in the tropics and mid-latitudes) and iii) an annually reconstruction of ENSO variability based on the North American Drought Atlas (Cook et al., 2004, Li et al., 2011).

130 2.3 Modelled $\delta^{18}\text{O}$ in precipitation and soil water

Beside the observational/reanalysis-based climate data, we also investigate the relation between $\delta^{18}\text{O}_{\text{cel}}$ and $\delta^{18}\text{O}_{\text{p}}/\delta^{18}\text{O}_{\text{SW}}$, as simulated by the water isotope enabled ECHAM5-wiso model (Werner et al., 2011) in order to get further insights regarding the correlation with other seasons and to identify a multi-seasonal climate signal. The $\delta^{18}\text{O}_{\text{p}}/\delta^{18}\text{O}_{\text{SW}}$ dataset was created in the study of Butzin et al. (2014) where they used the isotope-enabled version of the atmospheric general circulation model

135 ECHAM5 (Roeckner et al., 2003; Hagemann et al., 2006; Roeckner et al., 2006) which is called ECHAM5-wiso (Werner et al., 2011). In the study of Butzin et al. (2014), values of present-day insolation and greenhouse gas concentrations (Intergovernmental Panel on Climate Change, 2000) and monthly varying fields of sea-surface temperatures and sea-ice concentrations according to ERA-40 and ERA-Interim reanalysis data (Uppala et al., 2005; Berrisford et al., 2011; Dee et al., 2011) are used to force the model. To represent the climate conditions of the period 1960 to 2010, Butzin et al. (2014) used

140 an implicit nudging technique (Krishnamurti et al., 1991; the implementation in ECHAM is described by Rast et al., 2013). The nudging technique is a part of climate modelling sciences, where modelled fields of climate variables are relaxed to observations or data from reanalysis. In the study of Butzin et al. (2014), the modelled fields of surface pressure, temperature, divergence and vorticity are coupled to ERA-40 and ERA-Interim reanalysis fields (Uppala et al., 2005; Berrisford et al., 2011; Dee et al., 2011) for the period 1960 to 2010. The monthly grids of $\delta^{18}\text{O}_{\text{p}}/\delta^{18}\text{O}_{\text{SW}}$ have a horizontal

145 grid size of approximately $1.9^\circ \times 1.9^\circ$. Since our study is focused on seasonal variability, we have computed the seasonal averages for the $\delta^{18}\text{O}_{\text{p}}/\delta^{18}\text{O}_{\text{SW}}$ (DJF, MAM, JJA, SON).

2.4 Data analysis

As a first step, the characteristics of each time series of the $\delta^{18}\text{O}_{\text{cel}}$ network and their relation to altitude and latitude are investigated. For a better comparison, the linear trend of each $\delta^{18}\text{O}_{\text{cel}}$ time series is removed and the time series are

150 standardized (z-values).

To combine the signals of the isotope network, we use the Principle Component Analysis (PCA) and the Empirical Orthogonal Functions (EOF). These techniques were described by Pearson (1902) and Hotteling (1935) and were used for the first time by Lorenz (1956) for climatological studies (Storch and Zwiers, 1999). By applying the PCA, it is possible to extract a common climate signal from $\delta^{18}\text{O}_{\text{cel}}$ network which explains the highest part of the variability of the input dataset.

155 This is done by rotating the initial data onto axes which are orthogonal to each other (Schönwiese, 2013) by the corresponding eigenvectors. Therefore, the eigenvectors are used as a transformation matrix. The separate analysis of the eigenvector values is known as Empirical Orthogonal Functions (EOF). The goal of it is to identify the most dominant patterns of the $\delta^{18}\text{O}_{\text{cel}}$ tree network variability which explain a significant part of the variance for a specific region. The largest part of the variance can be explained by the pattern of the leading EOF. The temporal perspective on these patterns is

160 given by the principal components (PC) which describe the phase and the amplitude.

The resulting components are further checked if they fulfil the requirements of the rule of North et al. (1982). This rule states that the pattern of the eigenvectors of one component is strongly contaminated by other EOFs that correspond to the closest eigenvalues (Storch and Zwiers, 1999). To determine whether two consecutive patterns can be interpreted as distinct patterns, it is necessary to calculate the standard error in the estimation of the eigenvalues which is according to North et al. (1982) approximately

$$\Delta\lambda = \lambda \sqrt{2/n}$$

where λ is the eigenvalue and n the number of degrees of freedom of the data set. In case that the eigenvalues of two EOF's are not more separated from each other than this standard error, it is unlikely that the two consecutive patterns can be interpreted as distinct from each other, since any linear combination of the two eigenvectors is equally significant. In our study, we consider only that eigenvectors where the successive eigenvalues are distinguishable.

The ISONET network consists of a multi-site and multi-species tree-ring network covering more or less the period between 1600 to 2003. However, some tree-ring series cover the whole period, others cover only a shorter period. In order to be able to have a long-term perspective, one needs to find a statistically meaningful way to extend the shorter records to make use of the whole 400 years of data. Since most Multilinear Principal Component Analysis algorithms do not work with gaps in the initial matrix we make use of an algorithm developed by Josse and Husson (2016) which is able to fill the temporal gaps without a change of the PC. In the first step we place the mean in the gap and execute a PCA with this dataset. Afterwards, the dataset is projected onto the new component axis. So, that the values are rotated and the value of a gap change. The new value for the gap is placed into the initial dataset. With this new dataset, a PCA is again carried out. This process is repeated until convergence is reached. The result is a gap-free dataset which can be used for PCA. To quantify if our results are influenced by the gap filling method, we tested the correlation between PC1 based on the ISONET network and the first 4 PCs of the Old World Drought Atlas (OWDA; Cook et al., 2015) for the period 1850 to 2005 and 1600 to 2005. If the filling algorithm altered the representation of climate signals over a longer time period, we would expect that the strength of correlation is changing.

Composite maps of average precipitation, air temperature, geopotential height 500 mb (Z500) and SST are computed using years where the network's principle components are above or below a certain threshold. In our study, we choose maxima events above ($>\mu+\sigma$) and minima events below ($<\mu-\sigma$) one standard deviation (σ) with respect to the mean (μ). The composite maps allow us to analyse the general climate state occurring at times of minima (low) or maxima (high) separately. In addition, both composites of climate conditions can be combined under the assumption that the minima and maxima events show the opposite climate state. For this purpose, the minimum composite is subtracted from the maximum composite at each grid point (high-low). Beside the composite maps, we extract the values of PC1 for those years for which ENSO values are higher than the average plus one standard deviation and lower than the average minus one standard deviation. The difference from the former distribution for the values of minima and maxima years is tested with the t-test. To better understand if El Niño or La Niña events coevolve with extremes in the $\delta^{18}\text{O}_{\text{cel}}$ time series, the Event Coincidence

Analysis (ECA) (Donges et al., 2016; Siegmund et al., 2017) using PC1 and a December Nino 3.4 index is applied
195 (HadISST1; Rayner et al., 2003). The ECA quantifies the simultaneity of events contained in two series of observations
which can be computed with the R package CoinCalc (Siegmund et al., 2017). Furthermore, the CoinCalc package provides
functions to test if the coincidences are significant. In our study, we analyse whether the years in which the Nino 3.4 index is
above (below) the 75th (25th) percentile match the 75th (25th) percentile in PC1. In general, a significance level of $\alpha=0.05$ was
used in all analyses.

200 Finally, we analyse the relation between seasonally averaged $\delta^{18}\text{O}_\text{P}$ and $\delta^{18}\text{O}_\text{SW}$ from winter, spring and summer, based on
nudged ECHAM5-wiso simulations (Butzin et al., 2014), with PC1 based on the $\delta^{18}\text{O}_\text{cel}$ values from the ISONET network.
Our goal is to test the correlation between $\delta^{18}\text{O}_\text{cel}$ and modelled $\delta^{18}\text{O}_\text{P}/\delta^{18}\text{O}_\text{SW}$ to identify if the water, which is used within
the photosynthesis processes, has a multi-seasonal isotopic signature.

3 Results and Discussion

205 3.1 Characteristics of the $\delta^{18}\text{O}_\text{cel}$ network

The highest mean $\delta^{18}\text{O}_\text{cel}$ values occur at the southern locations, i.e. in Turkey and Carzola in Spain. For oaks and pines, the
lowest mean values are found for the northern sites (Fig. 2A). Moreover, generally lower $\delta^{18}\text{O}_\text{cel}$ values are identified for
Quercus compared to *Pinus*. Angiosperm wood tissue contains vessels, i.e. specialized water-conducting cells that are
generally larger in diameter, and therefore more conductive to water, than conifer wood cells (Sperry et al., 2006; Carnicer et
210 al., 2013). The overall variance of the datasets is not dependent on the type of tree species. The $\delta^{18}\text{O}_\text{cel}$ time series from
Poellau in Austria is characterized by the highest standard deviation whereas the time series from Lochwood in Great Britain
shows the lowest standard deviation.

Since the $\delta^{18}\text{O}$ source values and the fractionation processes are temperature dependent, it is necessary to evaluate the
influence of altitude and latitude for the oxygen isotope ratio. The relation of the $\delta^{18}\text{O}_\text{cel}$ values with regard to altitude and
215 latitude of each site is shown in Figs. 2B and 2C. In Fig. 2C, the linear relationship between the average $\delta^{18}\text{O}_\text{cel}$ values of the
locations and the corresponding latitudes are plotted. As shown by the boxplots of Fig. 2A, southern sample sites are
characterized by the highest average $\delta^{18}\text{O}_\text{cel}$ values whereas northern sites show the lowest average $\delta^{18}\text{O}_\text{cel}$ values. The
relation between the $\delta^{18}\text{O}_\text{cel}$ values and latitude is yielding a significant linear regression.

Beside the latitudinal effect, altitude also influences the oxygen isotope ratios as shown in Fig. 2B which can likewise be
220 described by a significant linear regression. It should be noted, that the southern sites are found at higher altitudes than the
northern sites, thus the latitudinal and altitudinal gradients may have confounding effects on $\delta^{18}\text{O}_\text{cel}$. Therefore, we show that
the $\delta^{18}\text{O}_\text{cel}$ network is influenced by a latitudinal and an altitudinal effect.

3.2 Characteristics of the principal components

225 Based on the EOF analysis, the first component of the isotope network explains 16.2%, the second 9.1%, the third 6.4%, the fourth 5.5%, and the fifth 5.2% of the variance. Therefore, the first five components explain a cumulative variability of around 43%. Since the first two components also fulfilled the requirements of the rule of North et al. (1982), they are investigated by their temporal and spatial characteristics.

230 The dominant pattern (EOF1), which describes 16.2% of the total variance, shows a spatially homogeneous structure (Fig. 3A). The majority of time series in Europe are characterized by negative eigenvector values. The pole of this EOF pattern is centred over France and Germany. In contrast, tree sites close to the Mediterranean Sea and the northernmost site in Finland are characterized by eigenvector values close to zero. Therefore, these locations contribute to a lesser extent to the first component's time series (PC1) shown in Fig. 3C. The time series of PC1 is characterized by an underlying negative trend from the 17th to the 18th century. From the beginning of the 18th century, a positive trend is observed until the beginning of the 19th century, where the highest values are reached. For the last 150 years, no clear trend is visible.

235 The second EOF (EOF2) is characterized by a completely different spatial pattern (Fig. 3B). Negative eigenvector values are found around the North and Baltic Sea, with the smallest eigenvector located in Norway, while positive eigenvector values are identified over the Southern/Southeast Europe and the Alpine region. The highest eigenvector values are recorded for the Italian site. In summary, this component highlights a dipole-like structure between Northern and Southern/Southeast Europe. This dipole-like structure is a well-known feature of the European hydroclimate (Ionita et al., 2015). The time series of the second component (PC2) is characterized by an underlying positive trend from the mid of the 19th century onwards. Furthermore, the highest interannual variability is found for the beginning of the 18th and 19th century. The highest values of the second component (PC2) are reached at the beginning of the 18th century, whereas the smallest values are identified for the beginning of the 19th century (Fig. 3 D).

245 Furthermore, we tested the correlation between PC1 and the first 4 PCs for the summer drought reconstruction based on the Old World Drought Atlas (OWDA; Cook et al., 2015) for the period 1850 to 2005, where we have the highest sample density. The highest correlation ($R=0.43$, $p\text{-value}=3.1e^{-08}$) is computed with PC2 of the OWDA (EOF plot and time series are shown in Supp. 2), which explains 16.1% of the total variance of the OWDA. If the filling algorithm altered the representation of climate signals over a longer time period, we would expect that the strength of correlation is also changing. Yet, the correlation is only slightly changing to Pearson's $R=0.39$ ($p\text{-value}=4.2e^{-16}$) for the entire period 1600 to 2005, which indicates that the filling algorithm does not impact the results. As a result, the climate signals obtained are robust and presented in a similar manner as for the period with a high sample coverage (i.e., 1850-2005). This argumentation is also supported by the comparison of the two time series in Supp. 2. We note that by using the gap filling method, uncertainties might arise for the first century where the sample density is low. It is, therefore, important to mention that the interpretation for the first century needs to be handled with care, and statements should be regarded as less robust.

3.3 Climate signals of PC1

For the winter season, high values of PC1 are associated with significant warm SSTs in the Equatorial Pacific and on the west coast of North and South America (Fig. 4A), which indicates that the high values of PC1 are co-evolving with the occurrence of the El Niño conditions. The strong signal in the Pacific persists throughout spring (Fig 4C) and reduces in summer (Fig 4E). A significant warming of the Tropical and North Atlantic is visible in spring and summer (Fig 4C, E). According to Latif and Grötzner (1999), the lagged warming of the Equatorial Atlantic can be observed up to 6 months after an El Niño event. In contrast, the Northeast Atlantic and the Mediterranean Sea are characterized by significantly colder SSTs in all three seasons. The low composite maps for PC1 and SST (Fig. 4B, D, F) show features of La Niña conditions associated with colder than average SSTs. This pattern is particularly prominent in the Tropical Pacific during winter and spring.

The related large-scale atmospheric circulation is shown in the composite map of Z500 (Fig. 5). During high values of PC1 which are co-evolving with the occurrence of El Niño conditions, the atmospheric circulation over Europe is characterized by a low-pressure regime in winter, whereas high-pressure regimes can be identified over the Northwest Atlantic as well as in the east of the low-pressure system (Fig. 5A). This fits well to the composite map of air temperature in Fig. 6B which shows significant cold conditions over the North Europe and significant warm conditions for Southeast Europe. The described temperature pattern shows similarities to the effects of a negative phase of the winter NAO. The opposite climate state can be observed for low values of PC1 in winter (Fig. 5B, 6B).

The atmospheric circulation remains in a similar configuration over Europe and the North Atlantic for low and high composite maps for spring (Fig. 5C, 5D) compared to the winter season (Fig. 5C, D). One important difference to the pre-season is that a pressure belt is visible between Europe and the Gulf of Maine in both maps.

The composite maps of Z500 for summer are characterized by a pressure regime centred over France and Germany (Fig. 5E, 5F). In both maps, it is visible that the low-/high-pressure regime in Central and Western Europe is surrounded by opposite pressure regimes. In case of a high-pressure system in the centre, it leads to a blocked zonal flow which is shown in Europe in Fig. 5F. The composite maps of precipitation and temperature are also supporting the analysis with the Z500 data. The climate of Central and Western Europe is characterized by significantly higher (lower) precipitation in Central Europe as well as significantly lower (higher) surface air temperatures in summer corresponding to low (high) $\delta^{18}\text{O}_{\text{cel}}$ values. The significant relation between PC1 and the summer hydroclimate is also resampled by the correlation between a SPEI3 index for JJA (Vicente-Serrano et al., 2010; Longitude -5° to 10° /Latitude 46° to 52°) and PC1. The correlation is significant ($R=0.49$; $p < 0.01$) for the period from 1901 to 2005 which suggests that PC1 can capture the hydroclimate variability in summer.

To further investigate the relation between ENSO variability and the PC1, we apply two different statistical approaches. The first approach is to analyse if El Niño and La Niña events are separated in the probability density plots of PC1. During El Niño years, the distribution of the PC1 is shifted towards higher values, whereas the opposite occurs during La Niña years

(see supplementary material; Fig. S3). According to the t-test, both shifts are significantly different compared to the distribution of PC1 ($p < 0.05$). The second statistical approach investigates if extremes in $\delta^{18}\text{O}_{\text{cel}}$ time series are co-occurring with El Niño or La Niña events. For this purpose, we apply the Event Coincidence Analysis (Siegmund et al., 2017; Donges et al., 2016) using PC1 and December Nino 3.4 index (HadISST1; Rayner et al., 2003). Over the period 1871-2005, 41.2% high and low extremes in the Nino 3.4 coincided significantly during winter, with high and low extremes of PC1 ($p < 0.01$). By extending the analysis period from 1750 to 1850, coincidence rates (28% % of the NDJ Nino 3.4 (Li et al., 2013) high and low extremes coincided not significantly ($p > 0.1$) during winter with high and low extremes of PC1) and also the correlations (Supp. 3) between PC1 and ENSO reconstructions Dätwyler et al. (2019) and Li et al. (2011, 2013) are weakening.

3.4 Comparison of $\delta^{18}\text{O}_{\text{cel}}$ with modelled $\delta^{18}\text{O}$ in precipitation and soil water

By employing nudged climate simulations with ECHAM5-wiso (Butzin et al., 2014), we evaluate how the $\delta^{18}\text{O}_{\text{cel}}$ tree signature is related to the modelled $\delta^{18}\text{O}$ in precipitation and soil water. A significant correlation between PC1 and the modelled $\delta^{18}\text{O}_{\text{p}}$ is shown in the correlation maps for winter, spring and summer, where Central Europe is characterized by a moderate correlation (Fig. 7A-C). A similar pattern can be identified for the correlation between $\delta^{18}\text{O}_{\text{sw}}$ and PC1. Compared to our previous analysis, the correlation between these quantities is increasing from winter to summer where it reached the maximum correlation (Fig. 7G). Since the $\delta^{18}\text{O}_{\text{cel}}$ ratio is largely dependent on $\delta^{18}\text{O}_{\text{sw}}$, the relation with $\delta^{18}\text{O}_{\text{sw}}$ is stronger compared to $\delta^{18}\text{O}_{\text{p}}$. Overall, the results of Fig. 5 indicate that significant correlations for both quantities can be computed for entire Europe except the eastern parts.

3.5 Further climate signals in $\delta^{18}\text{O}_{\text{cel}}$

Besides the multi-seasonal signal, the second component of the $\delta^{18}\text{O}_{\text{cel}}$ values significantly relates to the summer climate (Fig. 8, 9). A positive (negative) geopotential height anomaly in northern Europe with the centre over the North Sea co-occurs with a negative (positive) Z500 anomaly in Southeast Europe (Fig. 9). This coincides with low (high) temperature in Central and North Europa whereas Northeast Europe is characterised by high (low) temperature (Fig. 8A). The same pattern is also shown in the composite maps for precipitation where a similar pattern is presented (Fig. 8B). Based on these patterns, the temporal distribution of extremes in the PC2 time series, indicates that the 19th century has experienced increased drought in northern Europe and enhanced precipitation in the Adriatic region (Fig. 3D).

315 **4 Discussion**

4.1 Latitudinal and altitudinal dependence of the $\delta^{18}\text{O}_{\text{cel}}$ network

The $\delta^{18}\text{O}_{\text{cel}}$ ratio is affected by the isotopic composition of the source water ($\delta^{18}\text{O}_{\text{P}}$, $\delta^{18}\text{O}_{\text{SW}}$), which varies according to the latitude and altitude of the sample site (e.g., McCarroll and Loader, 2004). The latitudinal position has an influence on the $\delta^{18}\text{O}$ in the atmosphere because of the strong correlation between the temperature and the $\delta^{18}\text{O}$ composition of water vapour in the atmosphere (Dansgaard, 1964). In addition, Dansgaard (1964) has suggested that altitude have an influence on the $\delta^{18}\text{O}$ ratio which primarily results from the cooling of air masses as they ascend a mountain, accompanied by the rainout of the excess moisture (Gat, 2010).

The presented results show that there is a linear relationship between $\delta^{18}\text{O}_{\text{cel}}$ and site altitude (Figure 2B) and latitude (Figure 2C), which proofs the concept of the often-stated effects of latitude and altitude on the $\delta^{18}\text{O}_{\text{cel}}$ (McCarroll and Loader, 2004).

Therefore, our results are in line with other studies which have already proved that concept, e.g. Szejner et al. (2016).

The effects of altitude and latitude on the photosynthesis process are also visible for other tree-ring based proxies. For example, according to the studies of Körner et al. (1991), Marshall & Zhang (1994) and Dietendorf et al. (2010), there is a highly significant altitude effect on the tree carbon isotope composition ($\delta^{13}\text{C}$). Since temperature decreases with increasing altitude and the partial air pressure is approximately 21% lower at 2000 m than at sea level, Körner et al. (2007) have argued that these environmental conditions lead to a faster molecular gas diffusion at any given temperature.

However, the distribution of our sample sites across Europe indicate that the isotope network is spatially limited (Fig. 1). For instance, the time series from Central and Western Europe are overrepresented compared to the ones from Southeast and Northern Europe. In addition, it is imperative to extent the isotope network by collecting more $\delta^{18}\text{O}_{\text{cel}}$ records from Eastern Europe to improve the validity of our results for this region. Furthermore, the samples were not taken from trees growing at the same altitude, which is critical for identifying a latitudinal effect. In fact, the sampled trees in Southern Europe grew at higher altitudes (≥ 1600 m) compared to the other sample sites, which could also bias the $\delta^{18}\text{O}_{\text{cel}}$ ratio. It is, thereby, not viable to compare two adjacent sites located at different altitudes, and challenging to distinguish between latitude and altitude effects.

4.2 Links between ENSO and PC1

The presented results in subchapter 3.3 are an indicator that ENSO activity is influencing the climate signal of PC1. The reasons for this are the described warm/cold SST pattern in the Equatorial Pacific and on the west coast of North and South America which are associated with El Niño and La Niña events (Allan et al., 1996). Furthermore, the clear and significant separation between El Niño and La Niña events in probability density functions and the coincidence of high and low values of Nino 3.4 and PC1 support our argumentation.

345 Moreover, the described temperature pattern in Fig. 6B resembles the effects of the winter NAO (Fig. 6B). During the
negative phase of the NAO, North Europe experience cold and Southeast Europe warm conditions in winter. Studies based
on observations (Fraedrich and Müller, 1992; Fraedrich, 1994; Brönnimann et al., 2004; Pozo-Vazquez et al., 2005;
Brönnimann et al., 2007) and models (Merkel and Latif, 2002; Mathieu et al., 2004) have shown that ENSO variability can
influence the winter NAO. Their results showed that an El Niño event leads to a negative phase of the NAO. Based on our
350 argumentation, we suggest that high values of PC1 are co-evolving with the occurrence of the El Niño conditions and low
values of PC1 are co-evolving with the occurrence of La Niña conditions.

4.3 The stability of the ENSO signal in the isotope network

In our study, we test the correlation between ENSO and PC1 of the $\delta^{18}\text{O}_{\text{cel}}$ network with three different reconstructions (Li et
al., 2011; Li et al., 2013; Dätwyler et al., 2019) and for two different time periods (1750-1849, 1850-1949), which is shown
355 in Supp. 4. Despite the fact that the sample density of the isotope network is relatively high in these two periods, the
correlation between the PC1 and the ENSO reconstructions is weaker and not significant for the period 1750 to 1849. But
not only the correlation is getting weaker, also the correlation between a set of different ENSO reconstructions is getting
weaker in the 18th century which was shown for specific periods in Dätwyler et al. (2019). Furthermore, Dätwyler et al.
(2019) have found a consistent teleconnection pattern during the 18th century, which is different to the known teleconnection
360 pattern of ENSO in the instrumental period. Moreover, the 1850s mark the end of Little Ice Age (LIA) period, when ENSO
properties and its teleconnections changed significantly (Rimbu et al., 2003, Felis et al., 2018). Furthermore, modelling
studies (e.g. Henke et al., 2017) have also reported an increased frequency of El Niño during LIA due to southern
displacement of the Intertropical Convergence Zone.

A change of the ENSO characteristics would also have an influence on the teleconnection with the European climate. For
365 instance, Rimbu et al. (2003) have investigated coral time series from the northern Red Sea, and identified a nonstationary
relationship between the tropical Pacific and the European–Middle Eastern climate during the pre-instrumental period (see
also Supp. 5). An unstable relationship between ENSO variability and the climate of Europe is also found in studies based on
instrumental data (e.g., Fraedrich, 1994; Fraedrich and Müller, 1992; Pozo-Vázquez et al., 2005) or ocean-atmosphere
coupled models (e.g., Raible et al., 2004; Deser et al., 2006; Brönnimann, 2007). The temporally unstable relationship
370 between climate variables and ENSO is not only restricted to Europe, but also present in other regions of the planet (e.g.,
Álvarez et al., 2015).

Weak or inconclusive correlations between PC1 and ENSO reconstructions could also arise from the fact that the quality of
the ENSO reconstructions decreases which could be based on a too low number of samples (especially in first years of the
reconstruction period) and a non-stationarity of the used teleconnection (Batehup et al., 2015). Furthermore, ENSO
375 reconstructions are mostly trained within the last 150 years and used for time periods characterized by an absence of
instrumental data. Therefore, confident statements can only be made from 1850 onwards, since instrumental measurements

of different climate variables are available. Thus, the only possibility to test and analyse the teleconnection before 1850 is by using ENSO reconstructions.

Another reason for the decrease in correlation could be the change of the climate signal of $\delta^{18}\text{O}_{\text{cel}}$. It is important to consider that the climate signal is directly coupled to the limiting factor for tree growth. It is possible that the limiting factor changes over time, which would result in different responses to climate. Esper et al. (2017) have shown that the climate signals in $\delta^{18}\text{O}_{\text{cel}}$ and $\delta^{13}\text{C}_{\text{cel}}$ change during warm and cold periods for trees in Switzerland, and they proposed to split the calibration between these two periods or to use corresponding transfer models. Future research is therefore required to investigate the climate signal during warm and cold periods, as well as the influence on our PCA results. However, as discussed above, we can only suggest that the relationship between ENSO and the European climate may not be stable over time.

4.4 The winter climate signal in $\delta^{18}\text{O}_{\text{cel}}$

The exact mechanism through which the $\delta^{18}\text{O}_{\text{cel}}$ captures a climate signal of the pre-seasons is still debated. For example, Heinrich et al. (2013) mentioned that winters with very low temperatures may damage the cambium more than usually requiring a longer recovery period. Such winters may have a negative effect on the cambial activity and on the photosynthesis process. Furthermore, Vaganov et al. (1999) have shown that precipitation during winter can sustainably affect tree growth in the following year. Their findings are similar to Treydte et al. (2006), who have shown that $\delta^{18}\text{O}_{\text{cel}}$ can contain a winter signal. Treydte et al. (2006) further argued that depending on the root system, winter snow fall, and the characteristics of groundwater reservoirs, it is likely that trees use precipitation from the pre-seasons. Nevertheless, it is possible that winter climate conditions can also be memorized in $\delta^{18}\text{O}_{\text{cel}}$ through different climate feedback processes. For example, Ogi et al. (2003) highlighted that a positive NAO is frequently followed by higher pressures and warmer temperatures in Europe during the next summer. The authors suggested that SST, sea ice extensions and snow fall anomalies capture the winter climate conditions and influence the summer climate.

However, the oxygen isotope signal in cellulose depends primarily on the corresponding oxygen signal of the soil water and precipitation. According to Saurer et al. (2012), $\delta^{18}\text{O}_{\text{SW}}$ constitutes the average $\delta^{18}\text{O}$ input to the arboreal system over several precipitation events, and is modified by partial evaporation from the soil (depending on soil texture and porosity) and by a potential time lag, depending on rooting depth. Here we obtain the strongest correlations with $\delta^{18}\text{O}_{\text{P}}$ in winter, spring and summer (Fig. 7A, B, C). Because the correlations with $\delta^{18}\text{O}_{\text{SW}}$ are strongest in summer and autumn (Fig. 7G, H) and $\delta^{18}\text{O}_{\text{SW}}$ is the input of the arboreal system, we suggest that the isotopic signal of $\delta^{18}\text{O}_{\text{cel}}$ corresponds to an average over $\delta^{18}\text{O}_{\text{P}}$ events from winter, spring and summer, transferred via the $\delta^{18}\text{O}_{\text{SW}}$. It may also explain the reason behind the strong ENSO signal that $\delta^{18}\text{O}_{\text{cel}}$ is able to capture during winter. Moreover, it indicates the high potential of $\delta^{18}\text{O}_{\text{cel}}$ to capture climate signals even outside of the growing season.

4.5 Links between PC2 and large-scale atmospheric modes

In the composite maps for the PC2 (Fig. 9), we obtain a dipole structure between North Europe and the Mediterranean region. The dipole is characterized by a pressure anomaly centred on the North Sea, and which expands from the Northeast Atlantic to the Baltic Sea. Its counterpart is present in the northern Mediterranean region, especially in the area of Italy, northern parts of Greece and the Adriatic region.

The described pattern shows similarities to the summer European blocking pattern (Barnston & Livezey, 1997; Cassou et al., 2005) which is often associated with the Summer North Atlantic Oscillation (SNAO) (Hurrell & van Loon, 1997).

According to Cassou et al. (2005), 17.8% of the positive phase and 17.9% of the negative phase of the summer European blocking pattern influence the total summer weather regimes in Europe.

The summer European blocking pattern is a surrogate indicator for storm track activities. During the positive index phase, the storm track moves farther northwards (Folland et al. 2009; Lehmann & Coumou 2015). This results in a low storm activity over Northern Europe characterized by dry conditions, less cloudiness, high temperatures and a blocked cyclonic flow (Lehmann & Coumou 2015). On the other hand, the Mediterranean region is affected by lower temperatures and more precipitation. The opposite phenomenon can be identified for the negative index phase. Northern Europe experiences an enhanced storm activity through the southward movement of storm track over Northwest Europe (Folland et al. 2009; Lehmann & Coumou 2015), which leads to higher precipitation, higher cloudiness and lower temperatures. Whereas, the northern Mediterranean experiences dry and warm conditions. These predominant summer European blocking pattern features are well represented in our composite maps of precipitation and temperature for PC2 (Fig. 8). Based on temporal evolution of PC2, we suggest that there is a tendency towards a negative index phase starting at the beginning of the 20th century.

Beside the link to summer blocking activity in Europe, the geopotential height pattern is often used in another context. For example, Sillmann and Croci-Maspoli (2009) have shown that a positive geopotential height anomaly over the North Sea describes an atmospheric blocking-like pattern which relates to climate extremes like floods and droughts in the European mid-latitudes. Moreover, this circulation anomaly pattern has been identified as the main driver for extreme dry periods over the Eastern Mediterranean (Oikonomou et al., 2010; Rimbu et al., 2014; Ionita and Nagavciuc, 2020), and for summer air temperature variability in Greece (Xoplaki et al., 2003a, b).

5 Conclusions

We present here a $\delta^{18}\text{O}_{\text{cel}}$ isotope network from tree rings for the last 400 years which was used to investigate the large-scale climate teleconnections related to the European climate. According to our analysis, the climate signals of the network indicate that a link between the $\delta^{18}\text{O}$ variability and ENSO exists in winter, spring and summer. The investigation of the modelled $\delta^{18}\text{O}_{\text{SW}}/\delta^{18}\text{O}_{\text{P}}$ suggests that the summer signal still dominates $\delta^{18}\text{O}_{\text{cel}}$ but is partly influenced by lagged winter and spring precipitation signals. We argue that this is based on hydroclimatic feedback processes as well as characteristics of the

water reservoirs of the different sample sites. The ENSO signal is detected for the last 130 years. However, no significant
440 links can be deduced during the period 1750 to 1850 which is indicating that the relationship between ENSO and the
European climate could be not stable over time. The teleconnection changes between the tropical Pacific and Europe during
the pre-instrumental period were also identified by coral data (Rimbu et al., 2003). Further knowledge about a change of
teleconnections is essential because teleconnections have a remote climate impact on top of the current global warming.
445 Our study shows that the EOF2 is characterized by a dipole pattern between North and Southeast Europe which is
comparable to the characteristics of the summer European blocking pattern. Since this mode is highly relevant for the
summer climate conditions on the entire European continent, the temporal perspective gives new insights about how the
frequency of this mode changed through time. Our findings suggest that there is a tendency towards a situation whereby
Southeast Europe is predominantly characterized by a high-pressure system and North Europe by a low-pressure system
starting at the beginning of the 20th century. The described pressure pattern is relevant for the society because it can
450 influence the spatial and frequency characteristics of climate extremes.

In the context of the ongoing discussion about the anthropogenic climate change, water isotope records can provide useful
information about spatial and frequency changes of specific large-scale atmospheric circulation patterns. As a logical next
step, more high-resolution paleoclimate data as well as comprehensive model simulations are required to provide additional
insights into the stationarity of reconstructed European climate signals and their stationarity in teleconnections.

455 Acknowledgements

D.B. and D.C. are funded by the PalEX Project (AWI Strategy Fund) and M.I. is funded by the REKLIM project. All but
four tree-ring stable isotope chronologies were established within the project ISONET supported by the European Union
(EVK2-CT-2002-00147 'ISONET'). We want to thank all participants of the ISONET project (L. Andreu, Z. Bednarsz, F.
Berninger, T. Boettger, C. M. D'Alessandro, J. Esper, N. Etien, M. Filot, D. Frank, M. Grabner, M. T. Guillemain, E.
460 Gutierrez, M. Haupt, E. Hidasvuori, H. Jungner, M. Kalela-Brundin, M. Krapiec, M. Leuenberger, H.H. Leuschner, N. J.
Loader, V. Masson-Delmotte, A. Pazdur, S. Pawelczyk, M. Pierre, O. Planells, R. Pukiene, C. E. Reynolds-Henne, K. T.
Rinne, A. Saracino, M. Saurer, E. Sonninen, M. Stievenard, V. R. Switsur, M. Szczepanek, E. Szychowska-Krapiec, L.
Todaro, K. Treydte, J. S. Waterhouse, and M. Weigl). The data from Turkey, Slovenia and Southwest Germany were
produced with the EU-funded project MILLENNIUM (GOCE 017008-2'MILLENNIUM'), special thanks to T. Levanic and
465 R. Touchan. The tree-ring stable isotope chronologies from Bulgaria were established with support of the German Research
Foundation DFG (HE3089-1, GR 1432/11-1) and in cooperation with the administration of Pirin National Park, Bulgaria.
Additionally, we want to thank M. Butzin and M. Werner for providing the $\delta^{18}\text{O}$ in precipitation and soil water from nudged
ECHAM5-wiso simulations and two anonymous reviewers for their helpful comments.

Data availability

470 The ISONET network is not publicly available. The time series of the individual sample sites can be request by the corresponding authors of the mentioned studies in subsection 2.1. The used climate datasets are publicly available, please check the references and links in subsection 2.2 for more details.

Author contributions

475 DB undertook the research, writing and analysis. MI, MW, GH, GS, NR, MF, IH, DC and GL supported DB in writing, data analysis and research approaches. GH, GS and IH were involved in the ISONET project. GL and MI are the PhD supervisors of DB.

Competing interests

The authors declare that there is no conflict of interest.

References

- 480 Allan, R. J., Lindesay, J. and Parker, D. E.: El Niño, southern oscillation & climatic variability, CSIRO, Collingwood, Vic., Australia., 1996.
- Álvarez, C., Veblen, T. T., Christie, D. and González-Reyes, Á.: Relationships between climate variability and radial growth of *Nothofagus pumilio* near altitudinal treeline in the Andes of northern Patagonia, Chile, , doi:[10.1016/J.FORECO.2015.01.018](https://doi.org/10.1016/J.FORECO.2015.01.018), 2015.
- 485 Andreu-Hayles, L., Ummenhofer, C. C., Barriendos, M., Schleser, G. H., Helle, G., Leuenberger, M., Gutiérrez, E. and Cook, E. R.: 400 Years of summer hydroclimate from stable isotopes in Iberian trees, *Clim Dyn*, 49(1–2), 143–161, doi:[10.1007/s00382-016-3332-z](https://doi.org/10.1007/s00382-016-3332-z), 2017.
- Barbour, M. M.: Stable oxygen isotope composition of plant tissue: a review, *Functional Plant Biol.*, 34(2), 83–94, doi:[10.1071/FP06228](https://doi.org/10.1071/FP06228), 2007.
- 490 Barnston, A. G. and Livezey, R. E.: Classification, Seasonality and Persistence of Low-Frequency Atmospheric Circulation Patterns, *Mon. Wea. Rev.*, 115(6), 1083–1126, doi:[10.1175/1520-0493\(1987\)115<1083:CSAPOL>2.0.CO;2](https://doi.org/10.1175/1520-0493(1987)115<1083:CSAPOL>2.0.CO;2), 1987.

Batehup, R., McGregor, S. and Gallant, A. J. E.: The influence of non-stationary teleconnections on palaeoclimate reconstructions of ENSO variance using a pseudoproxy framework, *Climate of the Past*, 11(12), 1733–1749, doi:<https://doi.org/10.5194/cp-11-1733-2015>, 2015.

495 Berrisford, P., Kållberg, P., Kobayashi, S., Dee, D., Uppala, S., Simmons, A. J., Poli, P. and Sato, H.: Atmospheric conservation properties in ERA-Interim, *Quarterly Journal of the Royal Meteorological Society*, 137(659), 1381–1399, doi:[10.1002/qj.864](https://doi.org/10.1002/qj.864), 2011.

Brienen, R. J. W., Helle, G., Pons, T. L., Guyot, J.-L. and Gloor, M.: Oxygen isotopes in tree rings are a good proxy for Amazon precipitation and El Niño–Southern Oscillation variability, *PNAS*, 109(42), 16957–16962,

500 doi:[10.1073/pnas.1205977109](https://doi.org/10.1073/pnas.1205977109), 2012.

Brönnimann, S., Luterbacher, J., Staehelin, J., Svendby, T. M., Hansen, G. and Svenøe, T.: Extreme climate of the global troposphere and stratosphere in 1940–42 related to El Niño, *Nature*, 431(7011), 971, doi:[10.1038/nature02982](https://doi.org/10.1038/nature02982), 2004.

Brönnimann, S.: Impact of El Niño–Southern Oscillation on European climate, *Reviews of Geophysics*, 45(3), doi:<https://doi.org/10.1029/2006RG000199>, 2007.

505 Brönnimann, S., Xoplaki, E., Casty, C., Pauling, A. and Luterbacher, J.: ENSO influence on Europe during the last centuries, *Climate Dynamics*, 28(2–3), 181–197, doi:[10.1007/s00382-006-0175-z](https://doi.org/10.1007/s00382-006-0175-z), 2007.

Butzin, M., Werner, M., Masson-Delmotte, V., Risi, C., Frankenberg, C., Gribanov, K., Jouzel, J. and Zakharov, V. I.: Variations of oxygen-18 in West Siberian precipitation during the last 50 years, *Atmospheric Chemistry and Physics*, 14(11), 5853–5869, doi:[10.5194/acp-14-5853-2014](https://doi.org/10.5194/acp-14-5853-2014), 2014.

510 Carnicer, J., Barbeta, A., Sperlich, D., Coll, M. and Penuelas, J.: Contrasting trait syndromes in angiosperms and conifers are associated with different responses of tree growth to temperature on a large scale, *Front. Plant Sci.*, 4, doi:[10.3389/fpls.2013.00409](https://doi.org/10.3389/fpls.2013.00409), 2013.

Cassou, C., Terray, L. and Phillips, A. S.: Tropical Atlantic Influence on European Heat Waves, *Journal of Climate*, 18(15), 2805–2811, doi:[10.1175/JCLI3506.1](https://doi.org/10.1175/JCLI3506.1), 2005.

515 Compo, G. P., Whitaker, J. S., Sardeshmukh, P. D., Matsui, N., Allan, R. J., Yin, X., Gleason, B. E., Vose, R. S., Rutledge, G., Bessemoulin, P., Brönnimann, S., Brunet, M., Crouthamel, R. I., Grant, A. N., Groisman, P. Y., Jones, P. D., Kruk, M. C., Kruger, A. C., Marshall, G. J., Maugeri, M., Mok, H. Y., Nordli, Ø., Ross, T. F., Trigo, R. M., Wang, X. L., Woodruff, S. D. and Worley, S. J.: The Twentieth Century Reanalysis Project, *Quarterly Journal of the Royal Meteorological Society*, 137(654), 1–28, doi:[10.1002/qj.776](https://doi.org/10.1002/qj.776), 2011.

- 520 Cook, E., Woodhouse, C., Eakin, C. M., Meko, D. and Stahle, D.: Long-Term Aridity Changes in the Western United States, *Science*, doi:[10.1126/SCIENCE.1102586](https://doi.org/10.1126/SCIENCE.1102586), 2004.
- Cook, E. R., Seager, R., Kushnir, Y., Briffa, K. R., Büntgen, U., Frank, D., Krusic, P. J., Tegel, W., Schrier, G. van der, Andreu-Hayles, L., Baillie, M., Baittinger, C., Bleicher, N., Bonde, N., Brown, D., Carrer, M., Cooper, R., Čufar, K., Dittmar, C., Esper, J., Griggs, C., Gunnarson, B., Günther, B., Gutierrez, E., Haneca, K., Helama, S., Herzig, F., Heussner, K.-U., Hofmann, J., Janda, P., Kontic, R., Köse, N., Kyncl, T., Levanič, T., Linderholm, H., Manning, S., Melvin, T. M., Miles, D., Neuwirth, B., Nicolussi, K., Nola, P., Panayotov, M., Popa, I., Rothe, A., Seftigen, K., Seim, A., Svarva, H., Svoboda, M., Thun, T., Timonen, M., Touchan, R., Trotsiuk, V., Trouet, V., Walder, F., Ważny, T., Wilson, R. and Zang, C.: Old World megadroughts and pluvials during the Common Era, *Science Advances*, 1(10), e1500561, doi:[10.1126/sciadv.1500561](https://doi.org/10.1126/sciadv.1500561), 2015.
- 525
- 530 Craig, H.: Isotopic standards for carbon and oxygen and correction factors for mass-spectrometric analysis of carbon dioxide, *Geochimica et Cosmochimica Acta*, 12(1–2), 133–149, doi:[10.1016/0016-7037\(57\)90024-8](https://doi.org/10.1016/0016-7037(57)90024-8), 1957.
- Dansgaard, W.: Stable isotopes in precipitation, *Tellus*, 16(4), 436–468, doi:[10.1111/j.2153-3490.1964.tb00181.x](https://doi.org/10.1111/j.2153-3490.1964.tb00181.x), 1964.
- Dätwyler, C., Abram, N. J., Grosjean, M., Wahl, E. R. and Neukom, R.: El Niño–Southern Oscillation variability, teleconnection changes and responses to large volcanic eruptions since AD 1000, *International Journal of Climatology*, 39(5), 2711–2724, doi:[10.1002/joc.5983](https://doi.org/10.1002/joc.5983), 2019.
- 535
- Dee, D. P., Uppala, S. M., Simmons, A. J., Berrisford, P., Poli, P., Kobayashi, S., Andrae, U., Balmaseda, M. A., Balsamo, G., Bauer, P., Bechtold, P., Beljaars, A. C. M., van de Berg, L., Bidlot, J., Bormann, N., Delsol, C., Dragani, R., Fuentes, M., Geer, A. J., Haimberger, L., Healy, S. B., Hersbach, H., Hólm, E. V., Isaksen, L., Kållberg, P., Köhler, M., Matricardi, M., McNally, A. P., Monge-Sanz, B. M., Morcrette, J.-J., Park, B.-K., Peubey, C., de Rosnay, P., Tavolato, C., Thépaut, J.-N. and Vitart, F.: The ERA-Interim reanalysis: configuration and performance of the data assimilation system, *Quarterly Journal of the Royal Meteorological Society*, 137(656), 553–597, doi:[10.1002/qj.828](https://doi.org/10.1002/qj.828), 2011.
- 540
- Deser, C., Capotondi, A., Saravanan, R. and Phillips, A. S.: Tropical Pacific and Atlantic Climate Variability in CCSM3, , doi:[10.1175/JCLI3759.1](https://doi.org/10.1175/JCLI3759.1), 2006.
- Diefendorf, A. F., Mueller, K. E., Wing, S. L., Koch, P. L. and Freeman, K. H.: Global patterns in leaf ^{13}C discrimination and implications for studies of past and future climate, *Proceedings of the National Academy of Sciences*, 107(13), 5738–5743, doi:[10.1073/pnas.0910513107](https://doi.org/10.1073/pnas.0910513107), 2010.
- 545
- Domeisen, D. I. V., Garfinkel, C. I. and Butler, A. H.: The Teleconnection of El Niño Southern Oscillation to the Stratosphere, *Reviews of Geophysics*, doi:[10.1029/2018RG000596](https://doi.org/10.1029/2018RG000596), 2019.

- 550 Donges, J. F., Schleussner, C.-F., Siegmund, J. F. and Donner, R. V.: Event coincidence analysis for quantifying statistical interrelationships between event time series, *Eur. Phys. J. Spec. Top.*, 225(3), 471–487, doi:[10.1140/epjst/e2015-50233-y](https://doi.org/10.1140/epjst/e2015-50233-y), 2016.
- Epstein, S., Thompson, P. and Yapp, C. J.: Oxygen and Hydrogen Isotopic Ratios in Plant Cellulose, *Science*, 198(4323), 1209–1215, doi:[10.1126/science.198.4323.1209](https://doi.org/10.1126/science.198.4323.1209), 1977.
- 555 Esper, J., Carnelli, A. L., Kamenik, C., Filot, M., Leuenberger, M. and Treydte, K.: Spruce tree-ring proxy signals during cold and warm periods, *Dendrobiology*, 77, 3–18, doi:[10.12657/denbio.077.001](https://doi.org/10.12657/denbio.077.001), 2017.
- Etien, N., Daux, V., Masson-Delmotte, V., Mestre, O., Stievenard, M., Guillemin, M. T., Boettger, T., Breda, N., Haupt, M. and Perraud, P. P.: Summer maximum temperature in northern France over the past century: instrumental data versus multiple proxies (tree-ring isotopes, grape harvest dates and forest fires), *Climatic Change*, 94(3), 429–456, doi:[10.1007/s10584-008-9516-8](https://doi.org/10.1007/s10584-008-9516-8), 2009.
- 560 Farquhar, G. D. and Lloyd, J.: 5 - Carbon and Oxygen Isotope Effects in the Exchange of Carbon Dioxide between Terrestrial Plants and the Atmosphere, in *Stable Isotopes and Plant Carbon-water Relations*, edited by J. R. Ehleringer, A. E. Hall, and G. D. Farquhar, pp. 47–70, Academic Press, San Diego., 1993.
- Felis, T., Ionita, M., Rimbu, N., Lohmann, G. and Kölling, M.: Mild and Arid Climate in the Eastern Sahara-Arabian Desert During the Late Little Ice Age, *Geophysical Research Letters*, 45(14), 7112–7119, doi:[10.1029/2018GL078617](https://doi.org/10.1029/2018GL078617), 2018.
- 565 Folland, C. K., Knight, J., Linderholm, H. W., Fereday, D., Ineson, S. and Hurrell, J. W.: The Summer North Atlantic Oscillation: Past, Present, and Future, *J. Climate*, 22(5), 1082–1103, doi:[10.1175/2008JCLI2459.1](https://doi.org/10.1175/2008JCLI2459.1), 2009.
- Fraedrich, K.: An ENSO impact on Europe?, *Tellus A*, 46(4), 541–552, doi:[10.1034/j.1600-0870.1994.00015.x](https://doi.org/10.1034/j.1600-0870.1994.00015.x), 1994.
- Fraedrich, K. and Müller, K.: Climate anomalies in Europe associated with ENSO extremes, *International Journal of Climatology*, 12(1), 25–31, doi:[10.1002/joc.3370120104](https://doi.org/10.1002/joc.3370120104), 1992.
- 570 Franke, J., Valler, V., Brugnara, Y. and Brönnimann, S.: Ensemble Kalman Fitting Paleo-Reanalysis Version 2, World Data Center for Climate (WDCC) at DKRZ, 110329856760 Bytes, doi:[10.26050/WDCC/EKF400_V2.0](https://doi.org/10.26050/WDCC/EKF400_V2.0), 2020.
- Fritts, H.: *Tree Rings and Climate*, Elsevier., 2012.
- Gat, J.: *Isotope Hydrology: A Study of the Water Cycle*, World Scientific, London., 2010.

- 575 Hafner, P., McCarroll, D., Robertson, I., Loader, N. J., Gagen, M., Young, G. H., Bale, R. J., Sonninen, E. and Levanič, T.:
A 520 year record of summer sunshine for the eastern European Alps based on stable carbon isotopes in larch tree rings,
Clim Dyn, 43(3), 971–980, doi:[10.1007/s00382-013-1864-z](https://doi.org/10.1007/s00382-013-1864-z), 2014.
- Hagemann, S., Arpe, K. and Roeckner, E.: Evaluation of the Hydrological Cycle in the ECHAM5 Model, *J. Climate*, 19(16),
3810–3827, doi:[10.1175/JCLI3831.1](https://doi.org/10.1175/JCLI3831.1), 2006.
- 580 Harris, I., Osborn, T. J., Jones, P. and Lister, D.: Version 4 of the CRU TS monthly high-resolution gridded multivariate
climate dataset, *Sci Data*, 7(1), 109, doi:[10.1038/s41597-020-0453-3](https://doi.org/10.1038/s41597-020-0453-3), 2020a.
- Harris, I., Osborn, T. J., Jones, P. and Lister, D.: Version 4 of the CRU TS monthly high-resolution gridded multivariate
climate dataset, *Sci Data*, 7(1), 109, doi:[10.1038/s41597-020-0453-3](https://doi.org/10.1038/s41597-020-0453-3), 2020b.
- Haupt, M., Weigl, M., Grabner, M. and Boettger, T.: A 400-year reconstruction of July relative air humidity for the Vienna
region (eastern Austria) based on carbon and oxygen stable isotope ratios in tree-ring latewood cellulose of oaks (*Quercus*
585 *petraea* Matt. Liebl.), *Climatic Change*, 105(1–2), 243–262, doi:[10.1007/s10584-010-9862-1](https://doi.org/10.1007/s10584-010-9862-1), 2011.
- Heinrich, I., Touchan, R., Dorado Liñán, I., Vos, H. and Helle, G.: Winter-to-spring temperature dynamics in Turkey derived
from tree rings since AD 1125, *Climate Dynamics*, 41(7–8), 1685–1701, doi:[10.1007/s00382-013-1702-3](https://doi.org/10.1007/s00382-013-1702-3), 2013.
- Helama, S., Meriläinen, J. and Tuomenvirta, H.: Multicentennial megadrought in northern Europe coincided with a global El
Niño–Southern Oscillation drought pattern during the Medieval Climate Anomaly, *Geology*, 37(2), 175–178,
590 doi:[10.1130/G25329A.1](https://doi.org/10.1130/G25329A.1), 2009.
- Helama, S., Läänelaid, A., Raisio, J., Mäkelä, H. M., Hilasvuori, E., Jungner, H. and Sonninen, E.: Oak decline analyzed
using intraannual radial growth indices, $\delta^{13}\text{C}$ series and climate data from a rural hemiboreal landscape in southwesternmost
Finland, *Environ Monit Assess*, 186(8), 4697–4708, doi:[10.1007/s10661-014-3731-8](https://doi.org/10.1007/s10661-014-3731-8), 2014.
- 595 Helliker, B. R. and Griffiths, H.: Toward a plant-based proxy for the isotope ratio of atmospheric water vapor, *Global*
Change Biology, 13(4), 723–733, doi:[10.1111/j.1365-2486.2007.01325.x](https://doi.org/10.1111/j.1365-2486.2007.01325.x), 2007.
- Hilasvuori, E., Berninger, F., Sonninen, E., Tuomenvirta, H. and Jungner, H.: Stability of climate signal in carbon and
oxygen isotope records and ring width from Scots pine (*Pinus sylvestris* L.) in Finland, *Journal of Quaternary Science*, 24(5),
469–480, doi:[10.1002/jqs.1260](https://doi.org/10.1002/jqs.1260), 2009.
- 600 Hill, S. A., Waterhouse, J. S., Field, E. M., Switsur, V. R. and Rees, T. A.: Rapid recycling of triose phosphates in oak stem
tissue, *Plant, Cell & Environment*, 18(8), 931–936, doi:[10.1111/j.1365-3040.1995.tb00603.x](https://doi.org/10.1111/j.1365-3040.1995.tb00603.x), 1995.

- Hirahara, S., Ishii, M. and Fukuda, Y.: Centennial-Scale Sea Surface Temperature Analysis and Its Uncertainty, *Journal of Climate*, 27(1), 57–75, doi:[10.1175/JCLI-D-12-00837.1](https://doi.org/10.1175/JCLI-D-12-00837.1), 2014.
- Hotelling, H.: The most predictable criterion, *Journal of Educational Psychology*, 26(2), 139–142, doi:[10.1037/h0058165](https://doi.org/10.1037/h0058165), 1935.
- 605 Hurrell, J. and Van Loon, H.: Decadal variations in climate associated with the North Atlantic, *Climatic Change*, 36(3), 301–326, doi:[10.1023/A:1005314315270](https://doi.org/10.1023/A:1005314315270), 1997.
- Ineson, S. and Scaife, A. A.: The role of the stratosphere in the European climate response to El Niño, *Nature Geoscience*, 2(1), 32–36, doi:[10.1038/ngeo381](https://doi.org/10.1038/ngeo381), 2009.
- Intergovernmental Panel on Climate Change, Ed.: Special report on emissions scenarios: a special report of Working Group III of the Intergovernmental Panel on Climate Change, Cambridge University Press, Cambridge; New York., 2000.
- 610 Ionita, M., Boroneanț, C. & Chelcea, S. Seasonal modes of dryness and wetness variability over Europe and their connections with large scale atmospheric circulation and global sea surface temperature. *Clim Dyn* 45, 2803–2829 (2015). <https://doi.org/10.1007/s00382-015-2508-2>
- Ionita, M. and Nagavciuc, V.: Forecasting low flow conditions months in advance through teleconnection patterns, with a special focus on summer 2018, *Scientific Reports*, 10(1), 13258, doi:[10.1038/s41598-020-70060-8](https://doi.org/10.1038/s41598-020-70060-8), 2020.
- 615 Josse, J. and Husson, F.: missMDA : A Package for Handling Missing Values in Multivariate Data Analysis, *Journal of Statistical Software*, 70(1), doi:[10.18637/jss.v070.i01](https://doi.org/10.18637/jss.v070.i01), 2016.
- Kahmen, A., Sachse, D., Arndt, S. K., Tu, K. P., Farrington, H., Vitousek, P. M. and Dawson, T. E.: Cellulose $\delta^{18}\text{O}$ is an index of leaf-to-air vapor pressure difference (VPD) in tropical plants, *Proc. Nat. Acad. Sci.*, 108(5), 1981–1986, doi:[10.1073/pnas.1018906108](https://doi.org/10.1073/pnas.1018906108), 2011.
- 620 King, M. P., Yu, E. and Sillmann, J.: Impact of strong and extreme El Niños on European hydroclimate, *Tellus A: Dynamic Meteorology and Oceanography*, 72(1), 1–10, doi:[10.1080/16000870.2019.1704342](https://doi.org/10.1080/16000870.2019.1704342), 2020.
- Körner, C.: The use of ‘altitude’ in ecological research, *Trends in Ecology & Evolution*, 22(11), 569–574, doi:[10.1016/j.tree.2007.09.006](https://doi.org/10.1016/j.tree.2007.09.006), 2007.
- 625 Körner, Ch., Farquhar, G. D. and Wong, S. C.: Carbon isotope discrimination by plants follows latitudinal and altitudinal trends, *Oecologia*, 88(1), 30–40, doi:[10.1007/BF00328400](https://doi.org/10.1007/BF00328400), 1991.

- Krishnamurti, T. N., Xue, J., Bedi, H. S., Ingles, K. and Oosterhof, D.: Physical initialization for numerical weather prediction over the tropics, *Tellus B*, 43(4), 53–81, doi:[10.1034/j.1600-0889.1991.t01-2-00007.x](https://doi.org/10.1034/j.1600-0889.1991.t01-2-00007.x), 1991.
- 630 Labuhn, I., Daux, V., Pierre, M., Stievenard, M., Girardclos, O., Féron, A., Genty, D., Masson-Delmotte, V. and Mestre, O.: Tree age, site and climate controls on tree ring cellulose $\delta^{18}O$: A case study on oak trees from south-western France, *Dendrochronologia*, 32(1), 78–89, doi:[10.1016/j.dendro.2013.11.001](https://doi.org/10.1016/j.dendro.2013.11.001), 2014.
- Labuhn, I., Daux, V., Girardclos, O., Stievenard, M., Pierre, M. and Masson-Delmotte, V.: French summer droughts since 1326 CE: a reconstruction based on tree ring cellulose delta O-18, *Climate of the Past*, 12(5), 1101–1117, doi:[10.5194/cp-12-1101-2016](https://doi.org/10.5194/cp-12-1101-2016), 2016.
- 635 Latif, M. and Grötzner, A.: The equatorial Atlantic oscillation and its response to ENSO, *Climate Dynamics*, 16(2–3), 213–218, doi:[10.1007/s003820050014](https://doi.org/10.1007/s003820050014), 2000.
- Lavergne, A., Daux, V., Villalba, R., Pierre, M., Stievenard, M., Vimeux, F. and Srur, A. M.: Are the oxygen isotopic compositions of *Fitzroya cupressoides* and *Nothofagus pumilio* cellulose promising proxies for climate reconstructions in northern Patagonia?, *Journal of Geophysical Research: Biogeosciences*, 121(3), 767–776, doi:[10.1002/2015JG003260](https://doi.org/10.1002/2015JG003260), 2016.
- 640 Lehmann, J. and Coumou, D.: The influence of mid-latitude storm tracks on hot, cold, dry and wet extremes, *Scientific Reports*, 5(1), doi:[10.1038/srep17491](https://doi.org/10.1038/srep17491), 2015.
- Li, J., Xie, S.-P., Cook, E. R., Huang, G., D’Arrigo, R., Liu, F., Ma, J. and Zheng, X.-T.: Interdecadal modulation of El Niño amplitude during the past millennium, *Nature Climate Change*, 1(2), 114–118, doi:[10.1038/nclimate1086](https://doi.org/10.1038/nclimate1086), 2011.
- 645 Li, J., Xie, S.-P., Cook, E. R., Morales, M. S., Christie, D. A., Johnson, N. C., Chen, F., D’Arrigo, R., Fowler, A. M., Gou, X. and Fang, K.: El Niño modulations over the past seven centuries, *Nature Climate Change*, 3(9), 822–826, doi:[10.1038/nclimate1936](https://doi.org/10.1038/nclimate1936), 2013.
- Lloyd-Hughes, B. and Saunders, M. A.: Seasonal prediction of European spring precipitation from El Niño–Southern Oscillation and Local sea-surface temperatures, *International Journal of Climatology*, 22(1), 1–14, doi:[10.1002/joc.723](https://doi.org/10.1002/joc.723), 2002.
- 650 Lorenz, E. N.: Empirical Orthogonal Functions and Statistical Weather Prediction, Massachusetts Institute of Technology, Department of Meteorology, Massachusetts., 1956.
- Marshall, J. D. and Zhang, J.: Carbon Isotope Discrimination and Water-Use Efficiency in Native Plants of the North-Central Rockies, *Ecology*, 75(7), 1887–1895, doi:[10.2307/1941593](https://doi.org/10.2307/1941593), 1994.

- 655 Mathieu, P.-P., Sutton, R. T., Dong, B. and Collins, M.: Predictability of Winter Climate over the North Atlantic European Region during ENSO Events, *J. Climate*, 17(10), 1953–1974, doi:[10.1175/1520-0442\(2004\)017<1953:POWCOT>2.0.CO;2](https://doi.org/10.1175/1520-0442(2004)017<1953:POWCOT>2.0.CO;2), 2004.
- McCarroll, D. and Loader, N. J.: Stable isotopes in tree rings, *Quaternary Science Reviews*, 23(7–8), 771–801, doi:[10.1016/j.quascirev.2003.06.017](https://doi.org/10.1016/j.quascirev.2003.06.017), 2004.
- 660 Merkel, U. and Latif, M.: A high resolution AGCM study of the El Niño impact on the North Atlantic/European sector, *Geophysical Research Letters*, 29(9), 5-1-5–4, doi:[10.1029/2001GL013726](https://doi.org/10.1029/2001GL013726), 2002.
- Nagavciuc, V., Ionita, M., Perşoiu, A., Popa, I., Loader, N. J. and McCarroll, D.: Stable oxygen isotopes in Romanian oak tree rings record summer droughts and associated large-scale circulation patterns over Europe, *Clim Dyn*, doi:[10.1007/s00382-018-4530-7](https://doi.org/10.1007/s00382-018-4530-7), 2018.
- 665 North, G. R., Bell, T. L., Cahalan, R. F. and Moeng, F. J.: Sampling Errors in the Estimation of Empirical Orthogonal Functions, *Mon. Wea. Rev.*, 110(7), 699–706, doi:[10.1175/1520-0493\(1982\)110<0699:SEITEO>2.0.CO;2](https://doi.org/10.1175/1520-0493(1982)110<0699:SEITEO>2.0.CO;2), 1982.
- Ogi, M., Tachibana, Y. and Yamazaki, K.: Impact of the wintertime North Atlantic Oscillation (NAO) on the summertime atmospheric circulation, *Geophysical Research Letters*, 30(13), doi:[10.1029/2003GL017280](https://doi.org/10.1029/2003GL017280), 2003.
- Oikonomou, C., Flocas, H. A., Hatzaki, M., Nisantzi, A. and Asimakopulos, D. N.: Relationship of extreme dry spells in Eastern Mediterranean with large-scale circulation, *Theor Appl Climatol*, 100(1), 137–151, doi:[10.1007/s00704-009-0171-4](https://doi.org/10.1007/s00704-009-0171-4), 670 2010.
- van Oldenborgh, G. J., Burgers, G. and Tank, A. K.: On the El-Niño Teleconnection to Spring Precipitation in Europe, *arXiv:physics/9812040* [online] Available from: <http://arxiv.org/abs/physics/9812040> (Accessed 29 October 2020), 1998.
- van Oldenborgh, J. and Burgers, G.: Searching for decadal variations in ENSO precipitation teleconnections, *Geophysical Research Letters*, 32(15), doi:[10.1029/2005GL023110](https://doi.org/10.1029/2005GL023110), 2005.
- 675 Pearson, K.: On lines and planes of closest fit to systems of points in space, *The London, Edinburgh, and Dublin Philosophical Magazine and Journal of Science*, 2(11), 559–572, doi:[10.1080/14786440109462720](https://doi.org/10.1080/14786440109462720), 1902.
- Porter, T. J., Pisaric, M. F. J., Field, R. D., Kokelj, S. V., Edwards, T. W. D., deMontigny, P., Healy, R. and LeGrande, A. N.: Spring-summer temperatures since AD 1780 reconstructed from stable oxygen isotope ratios in white spruce tree-rings from the Mackenzie Delta, northwestern Canada, *Clim Dyn*, 42(3–4), 771–785, doi:[10.1007/s00382-013-1674-3](https://doi.org/10.1007/s00382-013-1674-3), 2014.

- 680 Pozo-Vázquez, D., Gámiz-Fortis, S. R., Tovar-Pescador, J., Esteban-Parra, M. J. and Castro-Díez, Y.: El Niño–southern oscillation events and associated European winter precipitation anomalies, *International Journal of Climatology*, 25(1), 17–31, doi:[10.1002/joc.1097](https://doi.org/10.1002/joc.1097), 2005.
- Raible, C. C., Luksch, U. and Fraedrich, K.: Precipitation and Northern Hemisphere regimes, *Atmospheric Science Letters*, 5, 43–55, doi:[10.1016/j.atmoscilet.2003.12.001](https://doi.org/10.1016/j.atmoscilet.2003.12.001), 2004.
- 685 Rast, S., Brokopf, R., Cheedela, S.-K., Esch, M., Gayler, V., Kirchner, I., Kornblueh, L., Rhodin, A., Schmidt, H., Schulzweida, U. and Wieners, K.-H.: User manual for ECHAM6 - June 21, 2013, (2013-02-26), version echam-6.1.06p3-guide-1.3, , 220 S., doi:[10.17617/2.1810486](https://doi.org/10.17617/2.1810486), 2013.
- Rayner, N. A.: Global analyses of sea surface temperature, sea ice, and night marine air temperature since the late nineteenth century, *Journal of Geophysical Research*, 108(D14), doi:[10.1029/2002JD002670](https://doi.org/10.1029/2002JD002670), 2003.
- 690 Rinne, K. T., Loader, N. J., Switsur, V. R. and Waterhouse, J. S.: 400-year May–August precipitation reconstruction for Southern England using oxygen isotopes in tree rings, *Quaternary Science Reviews*, 60, 13–25, doi:[10.1016/j.quascirev.2012.10.048](https://doi.org/10.1016/j.quascirev.2012.10.048), 2013.
- Rimbu, N., Lohmann, G., Felis, T., and Pätzold, J., 2003: Shift in ENSO teleconnections recorded by a Red Sea coral. *J. Climate*, 16 (9), 1414-1422.
- 695 Rimbu, N., Dima, M., Lohmann, G. and Musat, I.: Seasonal prediction of Danube flow variability based on stable teleconnection with sea surface temperature, *Geophysical Research Letters*, 32(21), doi:[10.1029/2005GL024241](https://doi.org/10.1029/2005GL024241), 2005.
- Rimbu, N., G. Lohmann, M. Ionita, 2014: Interannual to multidecadal Euro-Atlantic blocking variability during winter and its relationship with extreme low temperatures in Europe. *J. Geophys. Res. Atmos.*, 119 (24), 13,621-13,636. doi:[10.1002/2014JD021983](https://doi.org/10.1002/2014JD021983).
- 700 Roden, J. S., Lin, G. and Ehleringer, J. R.: A mechanistic model for interpretation of hydrogen and oxygen isotope ratios in tree-ring cellulose, *Geochimica et Cosmochimica Acta*, 64(1), 21–35, doi:[10.1016/S0016-7037\(99\)00195-7](https://doi.org/10.1016/S0016-7037(99)00195-7), 2000.
- Roeckner, E., Bäuml, G., Bonaventura, L., Brokopf, R., Esch, M., Giorgetta, M., Hagemann, S., Kirchner, I., Kornblueh, L., Manzini, E., Rhodin, A., Schlese, U., Schulzweida, U. and Tompkins, A.: The atmospheric general circulation model ECHAM 5. PART I: Model description, , doi:[10.17617/2.995269](https://doi.org/10.17617/2.995269), 2003.

- 705 Roeckner, E., Brokopf, R., Esch, M., Giorgetta, M., Hagemann, S., Kornblueh, L., Manzini, E., Schlese, U. and Schulzweida, U.: Sensitivity of Simulated Climate to Horizontal and Vertical Resolution in the ECHAM5 Atmosphere Model, *Journal of Climate*, 19(16), 3771–3791, doi:[10.1175/JCLI3824.1](https://doi.org/10.1175/JCLI3824.1), 2006.
- Rozanski, K., Araguás-Araguás, L. and Gonfiantini, R.: Isotopic Patterns in Modern Global Precipitation, in *Climate Change in Continental Isotopic Records*, pp. 1–36, American Geophysical Union (AGU)., 2013.
- 710 Saurer, M., Borella, S., Schweingruber, F. and Siegwolf, R.: Stable carbon isotopes in tree rings of beech: climatic versus site-related influences, *Trees*, 11(5), 291, doi:[10.1007/s004680050087](https://doi.org/10.1007/s004680050087), 1997.
- Saurer, M., Cherubini, P., Reynolds-Henne, C. E., Treydte, K. S., Anderson, W. T. and Siegwolf, R. T. W.: An investigation of the common signal in tree ring stable isotope chronologies at temperate sites, *Journal of Geophysical Research: Biogeosciences*, 113(G4), doi:[10.1029/2008JG000689](https://doi.org/10.1029/2008JG000689), 2008.
- 715 Saurer, M., Kress, A., Leuenberger, M., Rinne, K. T., Treydte, K. S. and Siegwolf, R. T. W.: Influence of atmospheric circulation patterns on the oxygen isotope ratio of tree rings in the Alpine region, *Journal of Geophysical Research: Atmospheres*, 117(D5), doi:[10.1029/2011JD016861](https://doi.org/10.1029/2011JD016861), 2012.
- Saurer, M., Spahni, R., Frank, D. C., Joos, F., Leuenberger, M., Loader, N. J., McCarroll, D., Gagen, M., Poulter, B., Siegwolf, R. T. W., Andreu-Hayles, L., Boettger, T., Liñán, I. D., Fairchild, I. J., Friedrich, M., Gutierrez, E., Haupt, M., 720 Hilasvuori, E., Heinrich, I., Helle, G., Grudd, H., Jalkanen, R., Levanič, T., Linderholm, H. W., Robertson, I., Sonninen, E., Treydte, K., Waterhouse, J. S., Woodley, E. J., Wynn, P. M. and Young, G. H. F.: Spatial variability and temporal trends in water-use efficiency of European forests, *Global Change Biology*, 20(12), 3700–3712, doi:[10.1111/gcb.12717](https://doi.org/10.1111/gcb.12717), 2014.
- Schleser, G. H., Frenzel, B., Stauffer, B. and Weiss, M. M.: Parameters determining carbon isotope ratios in plants, *Problems of Stable Isotopes in Tree Rings, Lake Sediments and Peat Bogs as Climatic Evidence for the Holocene*, 725 *Paläoklimaforschung* 15, 71–95, 1995.
- Schönwiese, C.-D.: *Praktische Statistik für Meteorologen und Geowissenschaftler*, Borntraeger, Berlin., 2013.
- Schweingruber, F. H.: *Tree Rings and Environment Dendroecology*, Paul Haupt, Bern., 1996.
- Siegmund, J. F., Siegmund, N. and Donner, R. V.: CoinCalc—A new R package for quantifying simultaneities of event series, *Computers & Geosciences*, 98, 64–72, doi:[10.1016/j.cageo.2016.10.004](https://doi.org/10.1016/j.cageo.2016.10.004), 2017.
- 730 Sillmann, J. and Croci-Maspoli, M.: Present and future atmospheric blocking and its impact on European mean and extreme climate, *Geophysical Research Letters*, 36(10), doi:[10.1029/2009GL038259](https://doi.org/10.1029/2009GL038259), 2009.

- Sperry, J. S., Hacke, U. G. and Pittermann, J.: Size and function in conifer tracheids and angiosperm vessels, *American Journal of Botany*, 93(10), 1490–1500, doi:[10.3732/ajb.93.10.1490](https://doi.org/10.3732/ajb.93.10.1490), 2006.
- 735 Sternberg, L. and Deniro, M. J.: Isotopic Composition of Cellulose from C3, C4, and CAM Plants Growing Near One Another, *Science*, 220(4600), 947–949, doi:[10.1126/science.220.4600.947](https://doi.org/10.1126/science.220.4600.947), 1983.
- Storch, H. v and Zwiers, F. W.: *Statistical analysis in climate research*, Cambridge University Press, Cambridge ; New York., 1999.
- 740 Szejner, P., Wright, W. E., Babst, F., Belmecheri, S., Trouet, V., Leavitt, S. W., Ehleringer, J. R. and Monson, R. K.: Latitudinal gradients in tree ring stable carbon and oxygen isotopes reveal differential climate influences of the North American Monsoon System, *Journal of Geophysical Research: Biogeosciences*, 121(7), 1978–1991, doi:[10.1002/2016JG003460](https://doi.org/10.1002/2016JG003460), 2016.
- Treydte, K., Schleser, G. H., Helle, G., Frank, D. C., Winiger, M., Haug, G. H. and Esper, J.: The twentieth century was the wettest period in northern Pakistan over the past millennium, *Nature*, 440(7088), 1179–1182, doi:[10.1038/nature04743](https://doi.org/10.1038/nature04743), 2006.
- 745 Treydte, K., Schleser, G. H., Esper, J., Andreu, L., Bednarz, Z. and Berninger, F.: Climate signals in the European isotope network ISONET, *TRACE*, 5, 138–147, 2007a.
- 750 Treydte, K., Frank, D., Esper, J., Andreu, L., Bednarz, Z., Berninger, F., Boettger, T., D’Alessandro, C. M., Etien, N., Filot, M., Grabner, M., Guillemain, M. T., Gutierrez, E., Haupt, M., Helle, G., Hiltavuori, E., Jungner, H., Kalela-Brundin, M., Krapiec, M., Leuenberger, M., Loader, N. J., Masson-Delmotte, V., Pazdur, A., Pawelczyk, S., Pierre, M., Planells, O., Pukiene, R., Reynolds-Henne, C. E., Rinne, K. T., Saracino, A., Saurer, M., Sonninen, E., Stievenard, M., Switsur, V. R., Szczepanek, M., Szychowska-Krapiec, E., Todaro, L., Waterhouse, J. S., Weigl, M. and Schleser, G. H.: Signal strength and climate calibration of a European tree-ring isotope network, *Geophysical Research Letters*, 34(24), doi:[10.1029/2007GL031106](https://doi.org/10.1029/2007GL031106), 2007b.
- 755 Treydte, K., Boda, S., Graf Pannatier, E., Fonti, P., Frank, D., Ullrich, B., Saurer, M., Siegwolf, R., Battipaglia, G., Werner, W. and Gessler, A.: Seasonal transfer of oxygen isotopes from precipitation and soil to the tree ring: source water versus needle water enrichment, *New Phytologist*, 202(3), 772–783, doi:[10.1111/nph.12741](https://doi.org/10.1111/nph.12741), 2014.
- Trouet, V., Babst, F. and Meko, M.: Recent enhanced high-summer North Atlantic Jet variability emerges from three-century context, *Nature Communications*, 9(1), doi:[10.1038/s41467-017-02699-3](https://doi.org/10.1038/s41467-017-02699-3), 2018.

Uppala, S. M., KÅllberg, P. W., Simmons, A. J., Andrae, U., Bechtold, V. D. C., Fiorino, M., Gibson, J. K., Haseler, J.,
760 Hernandez, A., Kelly, G. A., Li, X., Onogi, K., Saarinen, S., Sokka, N., Allan, R. P., Andersson, E., Arpe, K., Balmaseda, M.
A., Beljaars, A. C. M., Berg, L. V. D., Bidlot, J., Bormann, N., Caires, S., Chevallier, F., Dethof, A., Dragosavac, M., Fisher,
M., Fuentes, M., Hagemann, S., Hólm, E., Hoskins, B. J., Isaksen, L., Janssen, P. A. E. M., Jenne, R., McNally, A. P.,
Mahfouf, J.-F., Morcrette, J.-J., Rayner, N. A., Saunders, R. W., Simon, P., Sterl, A., Trenberth, K. E., Untch, A., Vasiljevic,
D., Viterbo, P. and Woollen, J.: The ERA-40 re-analysis, *Quarterly Journal of the Royal Meteorological Society*, 131(612),
765 2961–3012, doi:[10.1256/qj.04.176](https://doi.org/10.1256/qj.04.176), 2005.

Vaganov, E. A., Hughes, M. K., Kirilyanov, A. V., Schweingruber, F. H. and Silkin, P. P.: Influence of snowfall and melt
timing on tree growth in subarctic Eurasia, *Nature*, 400(6740), 149–151, doi:[10.1038/22087](https://doi.org/10.1038/22087), 1999.

Vicente-Serrano, S. M., Beguería, S., López-Moreno, J. I., Angulo, M. and El Kenawy, A.: A New Global 0.5° Gridded
Dataset (1901–2006) of a Multiscalar Drought Index: Comparison with Current Drought Index Datasets Based on the Palmer
770 Drought Severity Index, *Journal of Hydrometeorology*, 11(4), 1033–1043, doi:[10.1175/2010JHM1224.1](https://doi.org/10.1175/2010JHM1224.1), 2010.

Vitas, A.: Tree-Ring Chronology of Scots Pine (*Pinus sylvestris* L.) for Lithuania, *BALTIC FORESTRY*, 14(2), 6, 2008.

Werner, M., Langebroek, P. M., Carlsen, T., Herold, M. and Lohmann, G.: Stable water isotopes in the ECHAM5 general
circulation model: Toward high-resolution isotope modeling on a global scale, *Journal of Geophysical Research:
Atmospheres*, 116(D15), doi:[10.1029/2011JD015681](https://doi.org/10.1029/2011JD015681), 2011.

775 Xoplaki, E., González-Rouco, J., Gyalistras, D., Luterbacher, J., Rickli, R. and Wanner, H.: Interannual summer air
temperature variability over Greece and its connection to the large-scale atmospheric circulation and Mediterranean SSTs
1950–1999, *Climate Dynamics*, 20(5), 537–554, doi:[10.1007/s00382-002-0291-3](https://doi.org/10.1007/s00382-002-0291-3), 2003a.

Xoplaki, E., González-Rouco, J. F., Luterbacher, J. and Wanner, H.: Mediterranean summer air temperature variability and
its connection to the large-scale atmospheric circulation and SSTs, *Climate Dynamics*, 20(7), 723–739, doi:[10.1007/s00382-
780 003-0304-x](https://doi.org/10.1007/s00382-003-0304-x), 2003b.

785

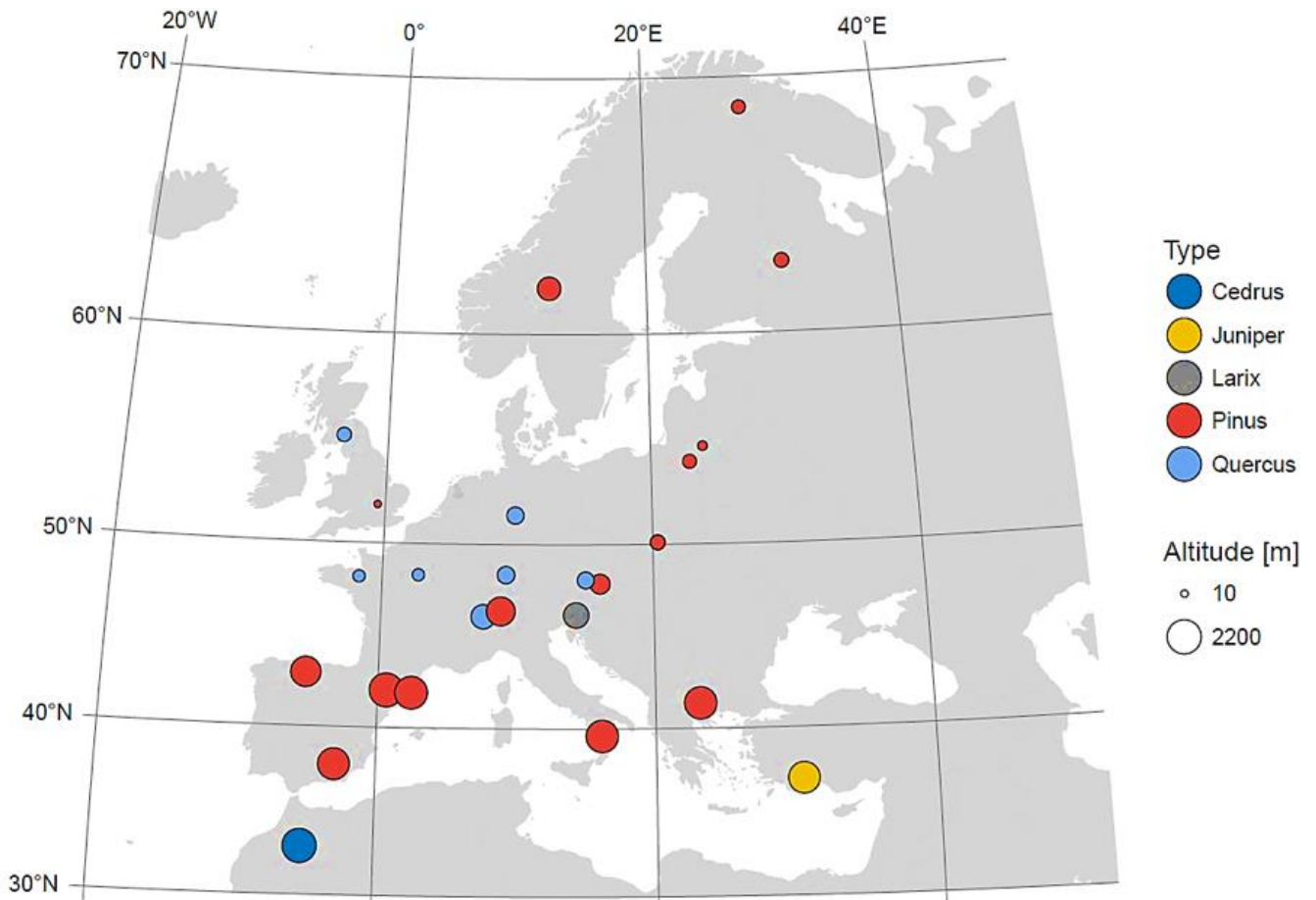


Figure 1: Spatial distribution of sample sites combined with the corresponding altitude. The highest density of sample sites exists in Central and Western Europe. The colour indicates the tree type (*Cedrus* (dark blue), *Juniper* (yellow), *Larix* (grey), *Pinus* (red) and *Quercus* (light blue)). The corresponding elevation (10-2200 m) is shown by the size of the circles.

790

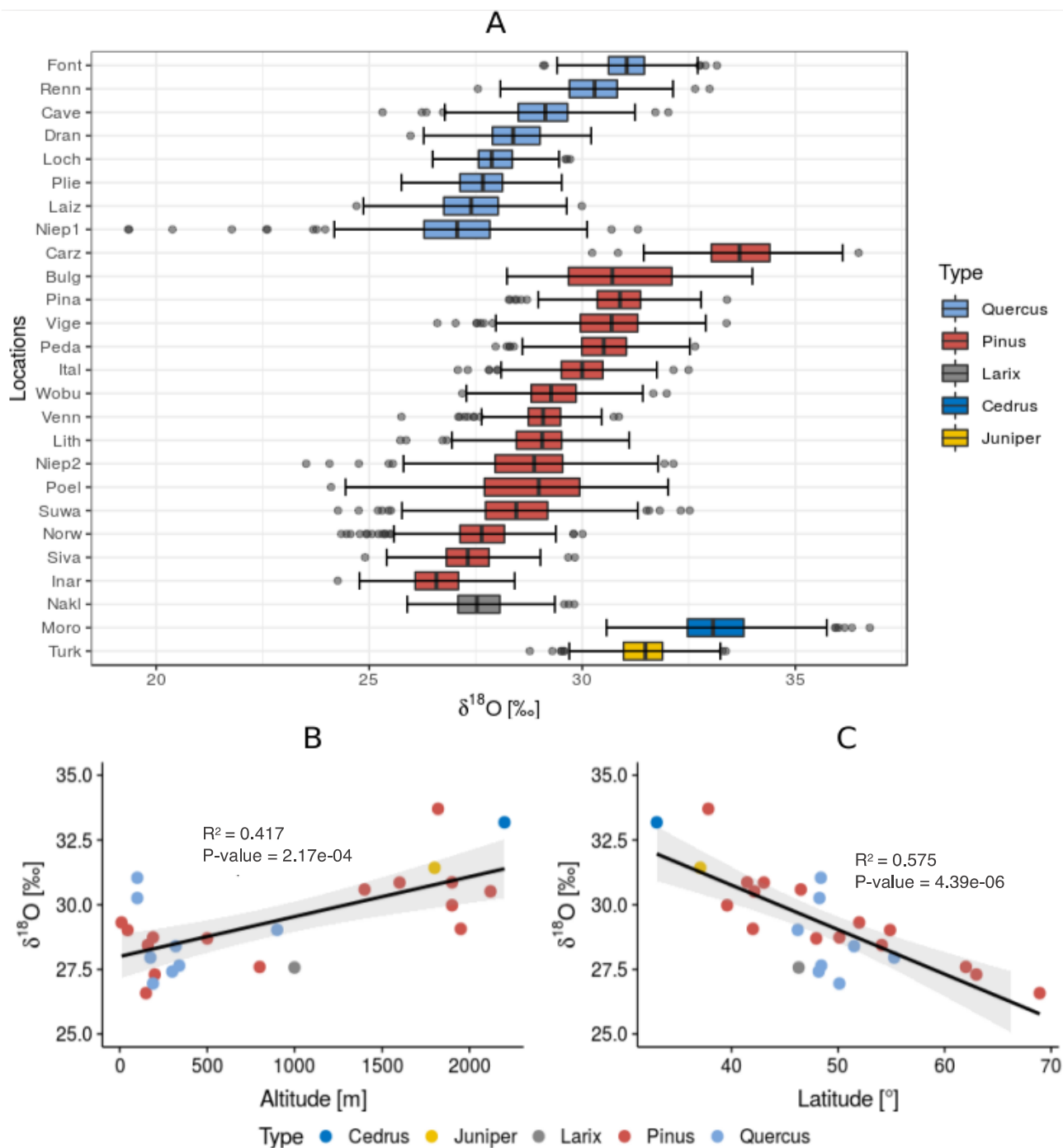


Figure 2: The characteristics of the European $\delta^{18}\text{O}$ time series/network. A, describes each time series with boxplots which were firstly ordered after the tree type and secondly after the average value. Additionally, the relation between the average value of each time series is plotted against their latitudinal (B) and their altitudinal position (C).

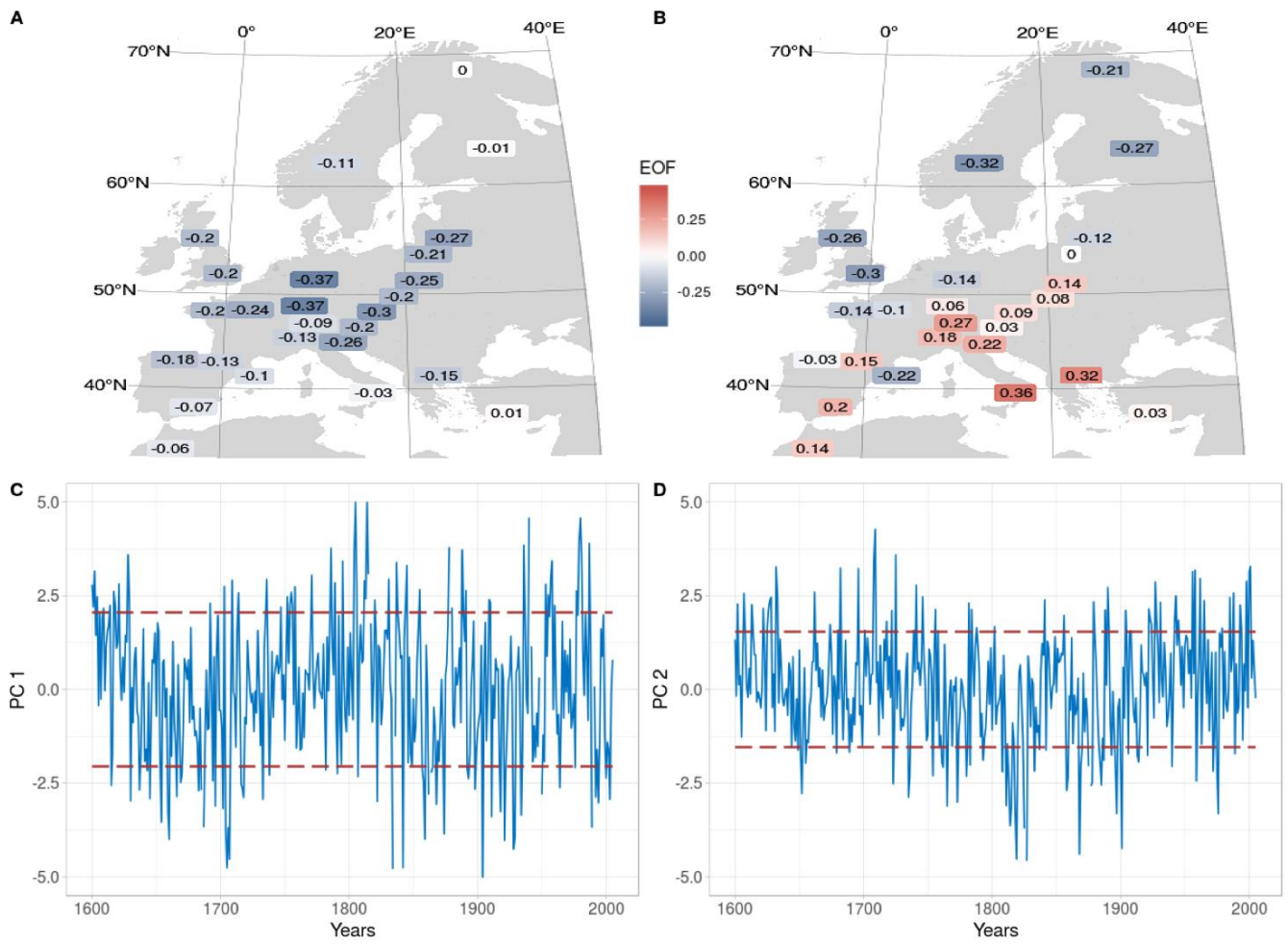


Figure 3: Spatial and temporal variability of the first two $\delta^{18}\text{O}$ components and EOFs. **A**, EOF for the first $\delta^{18}\text{O}$ component (16.2% explained variance), **B**, EOF for the second $\delta^{18}\text{O}$ component (9.5% explained variance). **C** and **D** are the time series for the first and second $\delta^{18}\text{O}$ component. The dashed red lines indicate the standard deviation for the years 1600-2005.

800

805

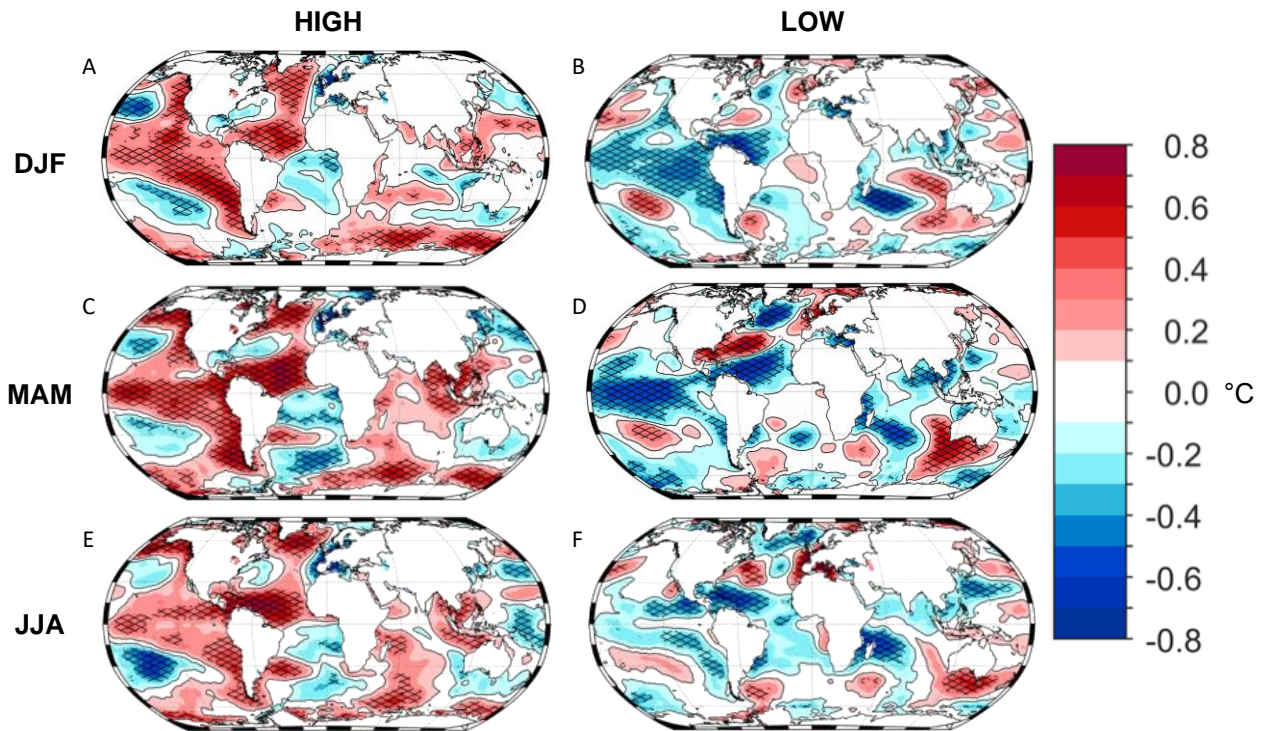
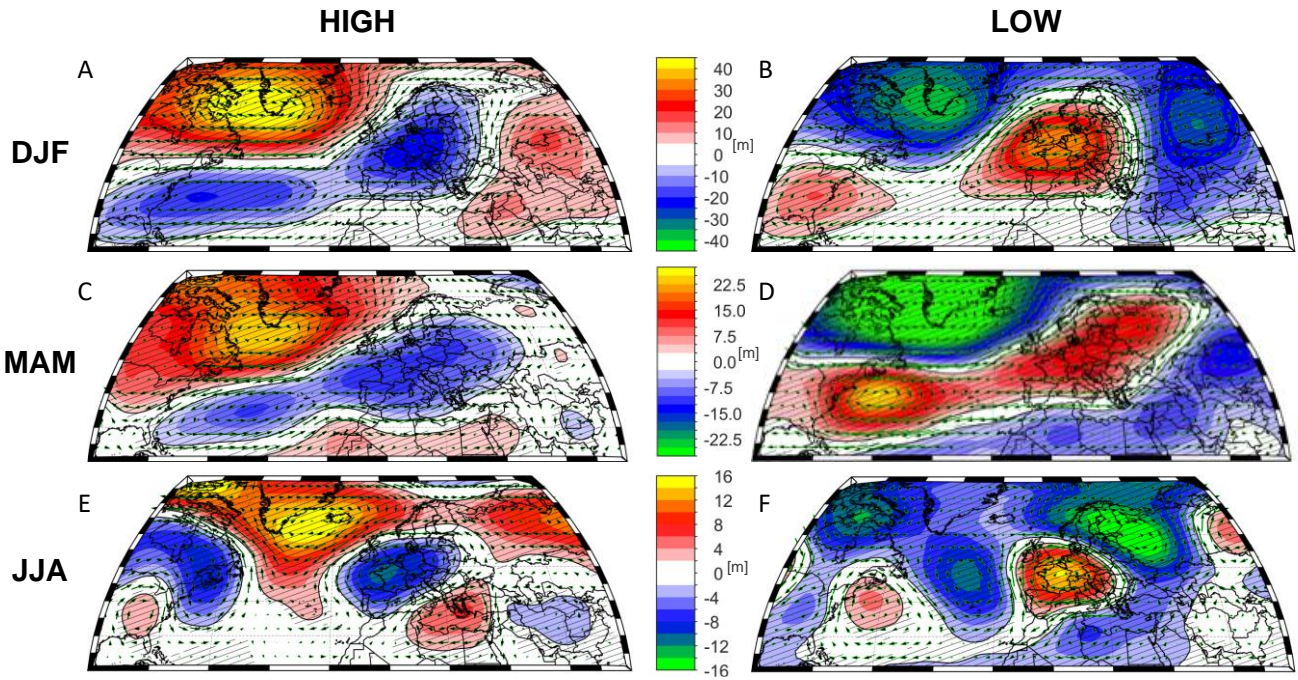


Figure 4: Composite maps (high and low) for SST related to the first $\delta^{18}\text{O}$ component for the seasons DJF, MAM and JJA. The first column shows the characteristics of the climate in DJF, the second in MAM and the third column in JJA, whereas the first row shows the results for maxima and the second for minima events of PC1. The SSTs in winter, spring and summer are characterized by ENSO activity. Furthermore, the significance is shown with a black grid in front of the colour. The SST dataset from ERSST (Huang et al., 2017) are included in this figure for the period 1854 to 2005.



820 **Figure 5: Composite maps (high and low) for Z500 related to the first $\delta^{18}\text{O}$ component for the seasons DJF, MAM and JJA. The**
 825 **first column shows the characteristics of the climate in DJF, the second in MAM and the third column in JJA, whereas the first row shows**
the results for maxima and the second for minima events of PC1. The Z500 maps show similar characteristics in winter and spring, whereas
a pressure regime is directly located over Central Europe in summer. The Z500 dataset from 20CRv2c (Compo et al., 2011) are used in
this figure for the period 1901 to 2005. Furthermore, the significance is shown with a black contour line.

830

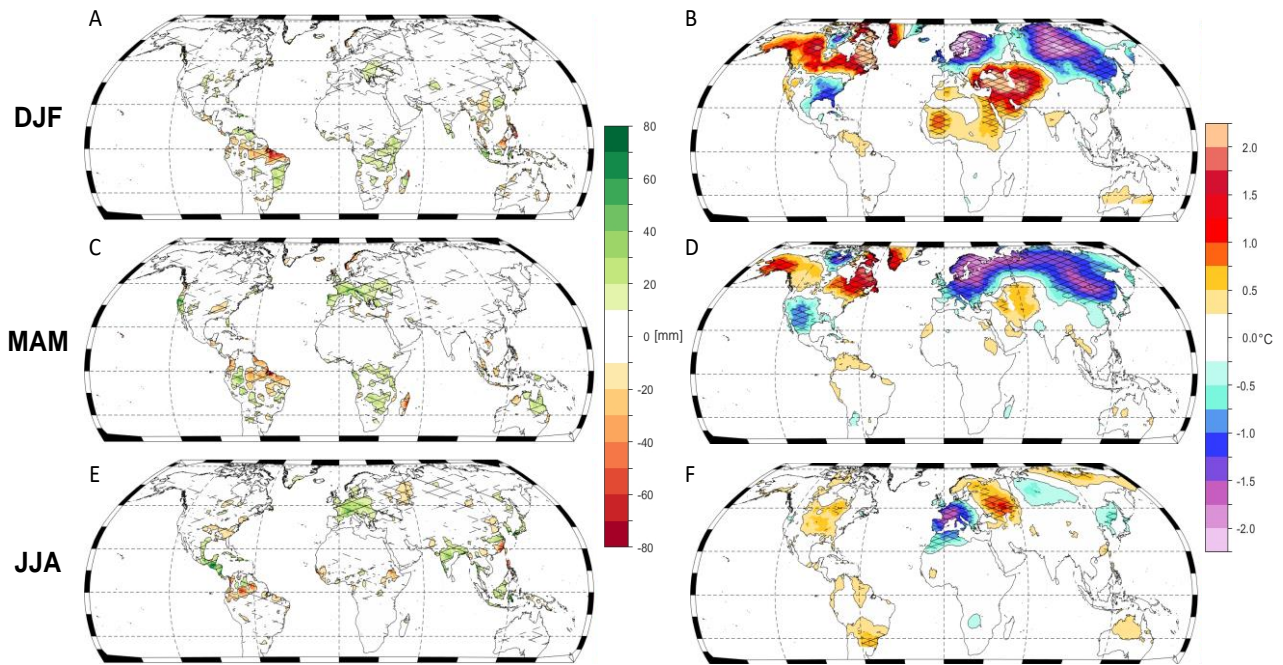


Figure 6: Composite maps (high-low) for precipitation and air temperature related to the first $\delta^{18}\text{O}$ component for the seasons DJF, MAM and JJA. The first column shows the characteristics of the climate in DJF, the second in MAM and the third column in JJA, whereas the first row shows the results for precipitation and the second for air temperature. The precipitation and air temperature dataset from CRU TS are included in this Figure for the period 1901 to 2005. The significance is shown with a black grid in front of the colour.

835

840

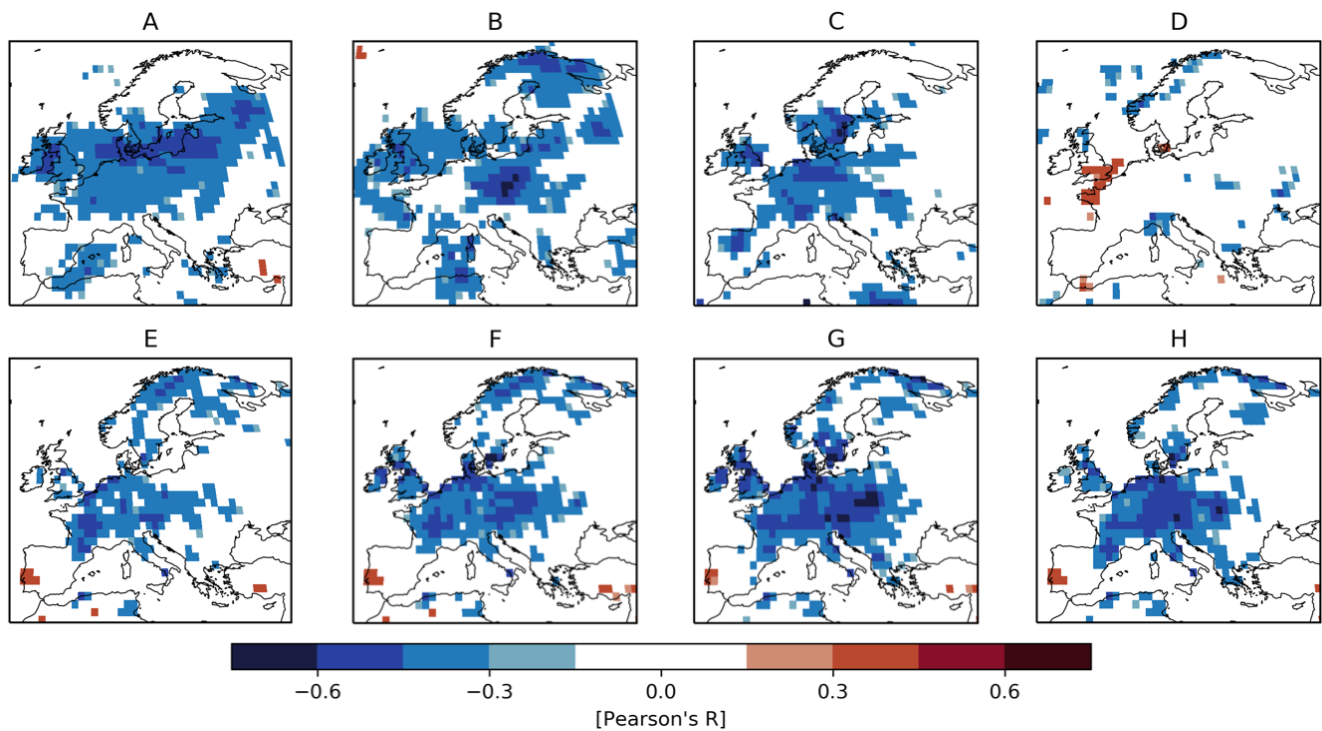


Figure 7: Links between the first $\delta^{18}\text{O}$ component and the modelled $\delta^{18}\text{O}$ in soil water and precipitation from nudged climate simulations with ECHAM5-wiso (Butzin et al., 2014). The upper row is showing the correlation between the first $\delta^{18}\text{O}$ component (PC1) and $\delta^{18}\text{O}$ in precipitation for winter (A), spring (B), summer (C) and autumn (D). Panels E, F, G, H are the correlation maps for PC1 and $\delta^{18}\text{O}$ in soil water for winter, spring, summer and autumn. In all maps, the significant grid cells are coloured.

845

850

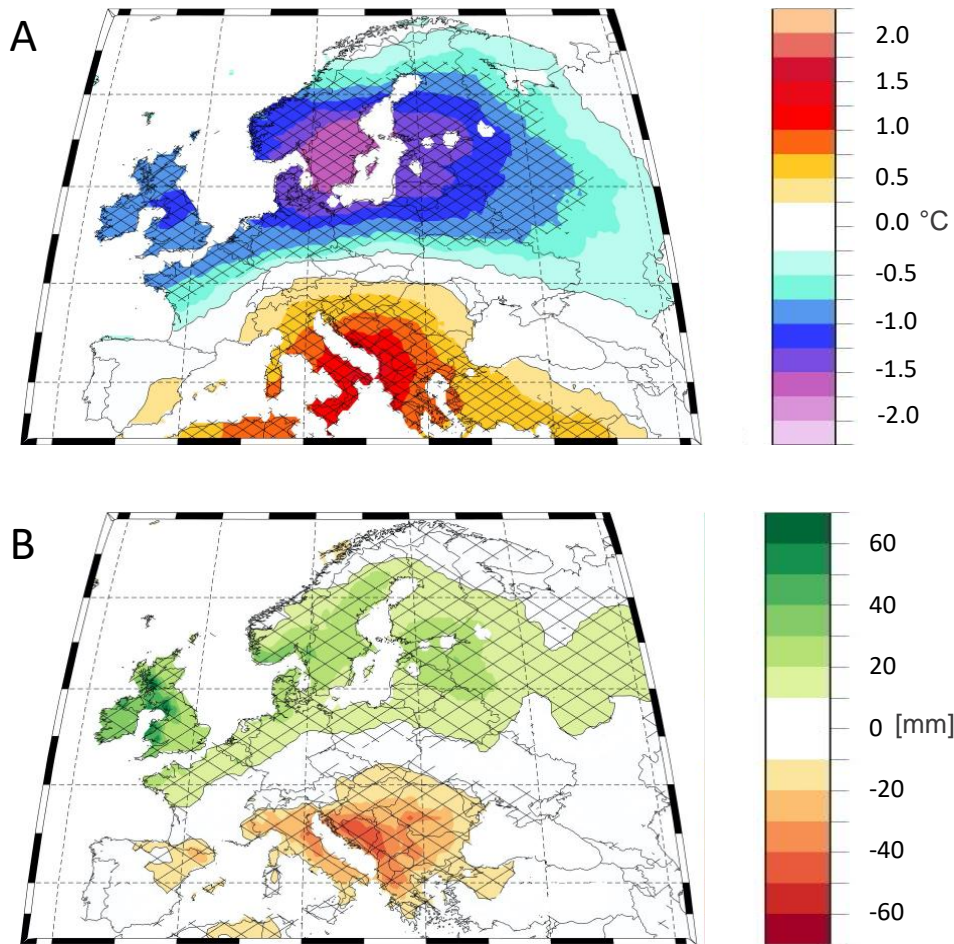


Figure 8: Composite maps (high-low) for the boreal summer related to the second $\delta^{18}\text{O}$ component. A, surface temperature JJA, B, precipitation JJA, C, Z500 JJA. The datasets are the same as in Figure 6. Furthermore, the significance is shown with a black grid in front of the colour.

855

860

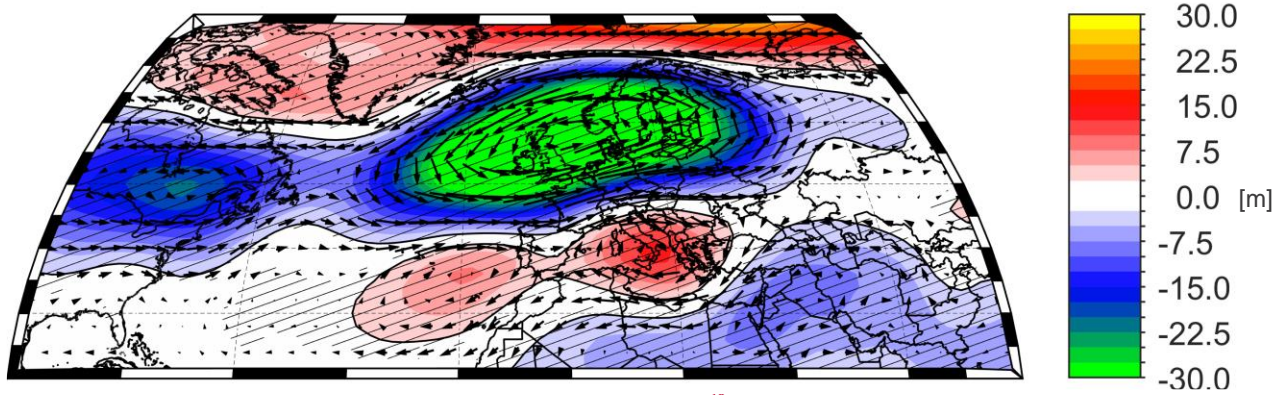


Figure 9: Composite map (high-low) for Z500 related to the second $\delta^{18}\text{O}$ component (PC2) for the boreal summer. The Z500 dataset from 20CRv2c (Compo et al., 2011) are used in this figure for the period 1901 to 2005. Furthermore, the significance is shown with a black contour line.

865